Open access • Posted Content • DOI:10.1101/2021.05.20.444848

Alum:CpG adjuvant enables SARS-CoV-2 RBD-induced protection in aged mice and synergistic activation of human elder type 1 immunity — Source link

Marisa McGrath, Robert Haupt, Hyuk-Soo Seo, Kijun Song ...+18 more authors

Institutions: University of Maryland, Baltimore, Harvard University, Ragon Institute of MGH, MIT and Harvard, University of Maryland Medical Center ...+1 more institutions

Published on: 20 May 2021 - bioRxiv (Cold Spring Harbor Laboratory)

Topics: CpG Oligodeoxynucleotide and TLR9

Title: Alum:CpG adjuvant enables SARS-CoV-2 RBD-induced protection in aged mice and synergistic activation of human elder type 1 immunity

One Sentence Summary: Alum and CpG enhance SARS-CoV-2 RBD protective immunity, variant neutralization in aged mice and Th1-polarizing cytokine production by human elder leukocytes.

Authors: Etsuro Nanishi[1, 2†], Francesco Borriello[1, 2, 3†], Timothy R. O'Meara[1‡], Marisa E. McGrath[4‡], Yoshine Saito[1], Robert E. Haupt[4], Hyuk-Soo Seo[5, 6], Simon D. van Haren[1, 2], Byron Brook[1, 2], Jing Chen[7], Joann Diray-Arce[1, 2], Simon Doss-Gollin[1], Maria De Leon[1], Katherine Chew[1], Manisha Menon[1], Kijun Song[5], Andrew Z. Xu[5], Timothy M. Caradonna[8], Jared Feldman[8], Blake M. Hauser[8], Aaron G. Schmidt[8, 9], Amy C. Sherman[1, 10], Lindsey R. Baden[10], Robert K. Ernst[11], Carly Dillen[4], Stuart M. Weston[4], Robert M. Johnson[4], Holly L. Hammond[4], Romana Mayer[12], Allen Burke[12], Maria E. Bottazzi[13, 14], Peter J. Hotez[13, 14], Ulrich Strych[13, 15], Aiquan Chang[16], Jingyou Yu[16], Dan H. Barouch[16], Sirano Dhe-Paganon[5, 6], Ivan Zanoni[2, 3], Al Ozonoff[1, 2], Matthew B. Frieman[4§], Ofer Levy[1, 2, 17§], David J. Dowling[1, 2§*]

Affiliations:

[1]*Precision Vaccines Program*, Division of Infectious Diseases, Boston Children's Hospital, Boston, MA, USA.

[2]Department of Pediatrics, Harvard Medical School, Boston, MA, USA.

[3]Division of Immunology, Boston Children's Hospital, Boston, MA, USA.

[4]Department of Microbiology and Immunology, University of Maryland School of Medicine, Baltimore, MD, USA.

[5]Department of Cancer Biology, Dana-Farber Cancer Institute, Boston, MA, USA.

[6]Department of Biological Chemistry and Molecular Pharmacology, Harvard Medical School, Boston, MA, USA.

[7]Research Computing Group, Boston Children's Hospital, Boston, MA, USA.

[8]Ragon Institute of MGH, MIT, and Harvard, Cambridge, MA, USA.

[9]Department of Microbiology, Harvard Medical School, Boston, MA, USA.

[10]Department of Medicine, Brigham and Women's Hospital, Boston, MA, USA.

[11]Department of Microbial Pathogenesis, University of Maryland School of Dentistry, Baltimore, MD, USA.

[12]Department of Pathology, University of Maryland Medical Center, Baltimore, MD, USA.

[13]Texas Children's Hospital Center for Vaccine Development, Baylor College of Medicine, Houston, TX, USA.

[14]National School of Tropical Medicine and Departments of Pediatrics and Molecular Virology & Microbiology, Baylor College of Medicine, Houston, TX, USA.

[15]National School of Tropical Medicine and Department of Pediatrics, Baylor College of Medicine, Houston, TX, USA.

[16]Center for Virology and Vaccine Research, Beth Israel Deaconess Medical Center, Harvard Medical School, Boston, MA, USA.

[17]Broad Institute of MIT & Harvard, Cambridge, MA, USA.

[†]These authors contributed equally to this manuscript.

‡These authors contributed equally to this manuscript.

§ Co-senior authors.

***Corresponding author**: David J. Dowling, *Precision Vaccines Program*, Division of Infectious Diseases, Boston Children's Hospital; Harvard Medical School, Rm 842, Boston, MA 02115, USA. Tel: +1 617-919-6890. e-mail: david.dowling@childrens.harvard.edu

ABSTRACT

Global deployment of vaccines that can provide protection across several age groups is still urgently needed to end the COVID-19 pandemic especially for low- and middle-income countries. While vaccines against SARS-CoV-2 based on mRNA and adenoviral-vector technologies have been rapidly developed, additional practical and scalable SARS-CoV-2 vaccines are needed to meet global demand. In this context, protein subunit vaccines formulated with appropriate adjuvants represent a promising approach to address this urgent need. Receptor-binding domain (RBD) is a key target of neutralizing antibodies (Abs) but is poorly immunogenic. We therefore compared pattern recognition receptor (PRR) agonists, including those activating STING, TLR3, TLR4 and TLR9, alone or formulated with aluminum hydroxide (AH), and benchmarked them to AS01B and AS03-like emulsion-based adjuvants for their potential to enhance RBD immunogenicity in young and aged mice. We found that the AH and CpG adjuvant formulation (AH:CpG) demonstrated the highest enhancement of anti-RBD neutralizing Ab titers in both age groups (~80-fold over AH), and protected aged mice from the SARS-CoV-2 challenge. Notably, AH:CpG-adjuvanted RBD vaccine elicited neutralizing Abs against both wild-type SARS-CoV-2 and B.1.351 variant at serum concentrations comparable to those induced by the authorized mRNA BNT162b2 vaccine. AH:CpG induced similar cytokine and chemokine gene enrichment patterns in the draining lymph nodes of both young adult and aged mice and synergistically enhanced cytokine and chemokine production in human young adult and elderly mononuclear cells. These data support further development of AH:CpG-adjuvanted RBD as an affordable vaccine that may be effective across multiple age groups.

INTRODUCTION

The coronavirus disease 2019 (COVID-19) pandemic caused by severe acute respiratory syndrome coronavirus 2 (SARS-CoV-2) resulted in a serious threat to humanity. Rapid deployment of safe and effective vaccines is proving key to reducing morbidity and mortality of COVID-19, especially in high-risk populations such as the older adults (*1*). Novel vaccine technologies including mRNA and adenoviral vector vaccines have dramatically accelerated the process of vaccine development, shown high efficacy in preclinical and clinical studies, and therefore been granted Emergency Use Authorization by the Food and Drug Administration (*2-9*). Unfortunately, worldwide access to these vaccines may be limited by the need for ultra-cold storage (mRNA vaccines), cost, and concerns regarding global scalability especially in the third world (*1*). This situation not only represents a major ethical problem but may also promote the emergence of vaccine-resistant SARS-CoV-2 strains due to high infection rates in unvaccinated regions (*10*). Thus, ongoing efforts are needed to investigate additional affordable, easily scalable, and effective vaccine approaches against SARS-CoV-2 to improve global access. To this end, alternative platforms such as inactivated and protein subunit SARS-CoV-2 vaccines have entered different stages of clinical development and in some cases have already been deployed at the population level (*11-17*). These approaches may play an essential role in the global fight against COVID-19 since they utilize well-established technologies, do not require low temperature storage, and have proven safety and effectiveness in various age groups including young children and the elderly.

With the exception of inactivated viruses, most SARS-CoV-2 vaccine candidates aim to target the SARS-CoV-2 Spike glycoprotein, as it is required for binding to the human receptor

angiotensin-converting enzyme 2 (ACE2) and subsequent cell fusion. In particular, the receptor-binding domain (RBD) of the Spike protein plays a key role in ACE2 binding and is targeted by many neutralizing antibodies (Abs) that exert a protective role against SARS-CoV-2 infection (*18-20*). RBD is an attractive candidate for a SARS-CoV-2 subunit vaccine and is relatively easy to produce at scale (*21, 22*); however, it is poorly immunogenic on its own. Structural biology-based vaccine design has been employed to overcome this limitation and has generated encouraging results in preclinical and clinical studies (*22-29*). A complementary approach to increase the immunogenicity of vaccine antigens consists of using adjuvants, which can enhance antigen immunogenicity by activating receptors of the innate immune system called pattern-recognition receptors (PRRs) and/or modulating antigen pharmacokinetics (*30, 31*). Adjuvant formulations of aluminum salts and PRR agonists enhance vaccine immune responses compared to aluminum salts or PRR agonists alone (*32*). AS04 was the first adjuvant system composed of aluminum salts and a PRR agonist, specifically the TLR4 agonist monophosphoryl lipid A (MPLA), to be included in a licensed human papillomavirus and hepatitis B vaccines (*32*). Thus, combinations of aluminum salts and PRR agonists represent a promising adjuvant platform to enhance RBD immunogenicity.

Here, we evaluated several combinations of PRR agonists and aluminum hydroxide (AH) and found that the TLR9 agonists CpG oligodeoxynucleotides formulated with AH and RBD dramatically enhanced immune response towards RBD in young mice using a prime-boost immunization schedule. The AH:CpG-adjuvanted RBD vaccine also elicited a robust anti-RBD immune response in aged mice, with the administration of an additional boost dose generating an anti-RBD Ab response comparable to young adult mice and providing complete protection from

121 live SARS-CoV-2 challenge. Overall, our comprehensive, head-to-head adjuvant comparison
122 study demonstrates that AH:CpG co-adjuvantation can overcome both the poor immunogenicity
123 of RBD and immunosenescence, supporting this approach for development of a scalable,
124 affordable, and safe global SARS-CoV-2 vaccine tailored for older adults.

RESULTS

Evaluation of multiple AH:PRR agonist formulations in young adult mice

We first evaluated whether distinct AH:PRR agonist formulations can overcome the low immunogenicity of monomeric RBD proteins. To this end, we performed a comprehensive comparison of PRR agonists, including 2'3'-cGAMP (stimulator of IFN genes (STING) ligand), Poly (I:C) (TLR3 ligand), PHAD (synthetic MPLA, TLR4 ligand), and CpG-ODN 2395 (TLR9 ligand). Each PRR agonist was formulated with and without AH. We also included AS01B (a liposome-based adjuvant containing MPLA and the saponin QS-21) as a clinical-grade benchmark adjuvant with potent immunostimulatory activity. The immunogenicity of vaccine formulations was first evaluated in 3-month-old young adult mice. Mice were immunized intramuscularly twice with 10 µg of monomeric RBD protein formulated with or without adjuvant, in a two-dose prime-boost regimen (Days 0 and 14). Two weeks after the boost immunization, humoral immune responses were evaluated. AH:PRR agonist formulations enhanced both anti-RBD Ab titers and inhibition of RBD binding to human ACE2 (hACE2) as compared to their respective non-AH adjuvanted formulations (**Fig 1A-C**). The Ab response elicited by AH alone was highly skewed to IgG1, with minimal inhibition of hACE2/RBD binding (**Fig 1D, E**). Among various AH:PRR agonist formulations, AH:CpG demonstrated the highest induction of total IgG, IgG1, and IgG2a along with a balanced IgG2a/IgG1 ratio (**Fig 1A-D**). Furthermore, the AH:CpG formulation significantly enhanced hACE2/RBD binding inhibition compared to all the other AH:PRR agonist formulations (**Fig 1E**). Abs induced by monomeric RBD immunization recognized the native trimeric Spike protein, as demonstrated by a binding ELISA with prefusion stabilized form of spike trimer (**Fig 1F**). To assess long-term immunogenicity, we then evaluated Ab responses and hACE2/RBD binding inhibition on Day

210 (**Fig 1G-J**). Of note, AH:CpG formulation maintained high hACE2/RBD binding inhibition while other adjuvant formulations waned their immune responses (**Fig 1E, J**).

AH:CpG-formulated RBD vaccine is immunogenic in aged mice

To assess the vaccine response in the context of aging, the immunogenicity of RBD vaccines adjuvanted with AH:PRR agonists was further studied in aged mice (14-month-old). Similar to young mice, the AH:CpG formulation also elicited the highest humoral immune response after prime-boost immunization in aged mice (**Fig 2A-F**). Of note, the vaccine adjuvanted with AH:CpG produced significantly higher hACE2/RBD inhibition and neutralizing titers compared to the vaccine adjuvanted with AS01B, which is known as a potent adjuvant in the human elderly population (*33, 34*) (**Fig 2E, F**). However, Ab levels were generally lower in aged mice, and the magnitude of the immune response of aged mice receiving the AH:CpG vaccine was significantly lower than that of young mice, suggesting an impaired vaccine response due to immunosenescence in the elderly population (**Fig S1**). To determine whether an additional dose can improve vaccine immunogenicity in aged mice, we administered a second booster dose two weeks after the last immunization. On Day 42 (two weeks after the 2^{nd} boost), enhancement in humoral responses was observed in AH:PRR agonist formulations (**Fig 2G-L**). Notably, a significant enhancement of hACE2/RBD inhibition was observed in aged mice receiving the two-boost AH:CpG vaccination regimen, with inhibition reaching the level of young mice that had received AH:CpG in a prime-boost regimen (**Fig S1**). High serum neutralizing Ab titers were observed in the AH:CpG and AS01B adjuvanted groups after the 2^{nd} boost but not in the non-adjuvanted nor AH alone-adjuvanted RBD groups. Assessment of cytokine production by splenocytes isolated from immunized mice and restimulated *in vitro* with Spike peptides

demonstrated high Th1 (IFNγ and IL-2) and low Th2 (IL-4) cytokine production in the AH:CpG and AS01B groups (**Fig 2M**). These results demonstrate that the AH:CpG-adjuvanted RBD vaccine is highly immunogenic in aged mice and an additional booster dose can further enhance anti-RBD humoral responses to match those observed in young mice.

AH:CpG-formulated RBD vaccine protects aged mice from lethal viral challenge

Neutralizing Abs are key to protecting from SARS-CoV-2 infection. Since RBD formulated with AH:CpG elicited high titers of neutralizing Abs, we assessed the protection of immunized mice in a challenge model. To this end, we employed the mouse-adapted SARS-CoV-2 MA10 virus strain (*35*). When tested in young (3-month-old) and aged (14-month-old) BALB/c mice, SARS-CoV-2 MA10 elicited dose-dependent weight loss (**Fig 3A, B**). Notably, aged mice challenged with 10^3 PFU or more exhibited dose-dependent mortality by 4 days post-infection (dpi) (**Fig 3C**). None of the young mice died by 4 dpi, including those that received the highest viral dose, in contrast with aged mice. Next, immunized aged mice were challenged with SARS-CoV-2 MA10 six weeks after the second boost. Bodyweight changes were assessed daily up to 4 dpi when the mice were sacrificed for viral titer and histopathology analyses. Aged mice immunized with the AH:CpG and AS01B adjuvanted vaccines showed no weight loss up to 4 dpi, whereas aged mice immunized with non-adjuvanted or AH-adjuvanted RBD showed rapid and significant bodyweight loss of >10% through 4 dpi (**Fig 4A**). Lung tissues were harvested and tested for SARS-CoV-2 viral titer in lung. No detectable live virus in lung tissues was observed in the AH:CpG and AS01B adjuvanted groups, while viral titers were detectable in the vehicle, non-adjuvanted, and AH-adjuvanted groups (**Fig 4B**). Histopathological analysis conducted in lung

193 tissues further confirmed the reduced SARS-CoV-2 infection in aged animals vaccinated with
194 AH:CpG and AS01B adjuvants (**Fig 4C, D**).
195
196 ***AH:CpG-formulated RBD and Spike mRNA vaccines elicit comparable levels of neutralizing***
197 ***antibodies against wild type SARS-CoV-2 and variants***
198 Recently, it has been reported that SARS-CoV-2 mRNA vaccines are more immunogenic than
199 RBD adjuvanted with oil-in-water emulsions (*36*). To assess whether this is a general feature of
200 RBD protein vaccines, we used the clinical-grade authorized BNT162b2 Spike mRNA vaccine
201 (Pfizer-BioNTech) as a benchmark and compared it to RBD formulated with AddaS03 (a
202 commercially available version of the oil-in-water emulsion AS03) and to AH:CpG in aged mice.
203 Along with CpG-2395, we also tested CpG-1018, which is included in the Heplisav-B vaccine
204 and has also been tested in combination with Spike/RBD and AH in SARS-CoV-2 studies
205 including human vaccine trials (*12, 16, 37*). In accordance with previously published data, the
206 mRNA vaccine was highly immunogenic, while RBD formulated with AddaS03 failed to induce
207 significant levels of neutralizing Abs (**Fig 5A-D**). Of note, both AH:CpG formulations elicited
208 levels of anti-RBD (**Fig 5A**), anti-Spike (**Fig 5B**) and neutralizing Abs (**Fig 5C, D**) comparable
209 to or greater than the mRNA vaccine.
210 SARS-CoV-2 variants such as B.1.1.7 and B.1.351 have emerged with reduced
211 neutralization from serum samples of convalescent or vaccinated individuals (*38-41*). A recent
212 report showed that the mRNA BNT162b2 vaccine maintained its effectiveness against severe
213 COVID-19 with the B.1.351 variant at greater than 90% (*42*). We therefore evaluated whether
214 RBD + AH:CpG and mRNA BNT162b2 vaccines elicit neutralizing Abs against these variants.
215 As expected, we observed reduced titers against the variants, especially against the B.1.351 (**Fig**

5E). The neutralization titers of RBD + AH:CpG decreased by 3.2-fold against B.1.351, and the mRNA BNT 162b2 decreased by 6.0-fold. Neutralizing titers against the B.1.351 were comparable between RBD + AH:CpG (GMT 382) and mRNA BNT162b2 (GMT 109).

Innate signaling potentiated by AH:CpG formulation is well preserved in aged mice

Lymph nodes (LNs) are critical sites for the interaction between innate and adaptive immune systems and orchestrate the development of vaccine immune responses (*43, 44*). Specifically, activation of the innate immune system can induce a rapid response in the LN characterized by LN expansion, which is driven by lymphocyte accrual and expression of proinflammatory molecules (*45, 46*). To gain further insights into the mechanism of action of the AH:CpG formulation, we collected draining LNs (dLNs) 24 hours post injection of AH:CpG or either adjuvant alone. CpG and AH:CpG induced comparable dLN expansion in both age groups (**Fig 6A**). To characterize the molecular events associated with these treatments further, RNA isolated from dLNs after injection of vehicle, CpG, or AH:CpG was subjected to a quantitative real-time PCR array comprised of 157 genes related to cytokines, chemokines, and type 1 IFN responses. Principal component analysis and hierarchical cluster analysis demonstrated a marked separation between AH and CpG-containing treatments, whereas similar patterns were observed between groups treated with AH:CpG and CpG alone in both age groups (**Fig 6B, C**). Generalized linear model analysis comparing gene expressions after AH, CpG, and AH:CpG treatments further revealed similar gene enrichment patterns between young adult and aged mice (**Fig 6D, E**). These results suggest that CpG and AH:CpG activate similar pathways in young and aged mice to elicit a LN innate response.

239 ***AH:CpG synergistically enhances proinflammatory cytokines from human elderly PBMCs***

240 In order to assess the translational relevance of an adjuvant formulation it is key to confirm its
241 ability to activate human immune cells. To this end, we stimulated human peripheral blood
242 mononuclear cells (PBMCs) isolated from young adults (18-40 years old) and elder adults (≥65
243 years old) with CpG, AH, and the admixed AH:CpG formulation and measured cytokine and
244 chemokine production. Whereas AH induced limited or no cytokine production, both CpG alone
245 and AH:CpG activated young adult and elderly PBMCs in a concentration-dependent manner
246 (**Fig 7A-D, Fig S2**). PBMCs of both age groups treated with AH:CpG produced significantly
247 higher levels of various proinflammatory cytokines and chemokines than those treated with CpG
248 alone (**Fig 7A-D**). Of note, CpG and AH synergistically induced IL-6, IL-10, TNF, CCL3, and
249 GM-CSF production in both young adult and elderly PBMCs, as defined mathematically (D
250 value, see Methods) (**Fig 7C, D, Fig S2**).

DISCUSSION

The risk of COVID-19-related morbidity and mortality increases with age (*47, 48*). Currently authorized SARS-CoV-2 vaccines have proven effective at preventing severe COVID-19 (*2-4*). Nevertheless, there is still the need to develop affordable and accessible vaccines that can provide protection across several age groups, especially for low- and middle-income countries (*1, 10, 49*). Protein subunit vaccines formulated with appropriate adjuvants represent a promising strategy to address this urgent need. Here, we performed a comprehensive head-to-head comparison of multiple adjuvants in age-specific *in vivo* and *ex vivo* animal models, along with age-specific human *in vitro* screening, to determine the appropriate adjuvant for a SARS-CoV-2 RBD vaccine in the young and the aged, focusing on the innate and humoral immune response reported to align best with known correlates of protection (*50, 51*). We found that the AH:CpG adjuvant formulation enhances anti-RBD neutralizing Ab titers and type 1 immunity (i.e. IgG2a switching, Th1 polarization) in both age groups. Aged mice immunized with AH:CpG are protected from live SARS-CoV-2 challenge. Of note, RBD adjuvanted with AH:CpG elicited levels of neutralizing Abs comparable to the clinical-grade BNT162b2 Spike mRNA vaccine. The translational relevance of our findings is also highlighted by the synergistic activation of human PBMCs from older individuals upon stimulation with AH:CpG. Overall, our results expand upon recent preclinical and clinical studies on the enhanced immunogenicity of Spike formulated with AH:CpG by showing that a vaccine composed of RBD and AH:CpG can also induce a robust anti-SARS-CoV-2 immune response across different age groups. Since an RBD antigen is amenable to high-yield manufacturability (*52-54*), our study also supports the development of RBD formulated with AH:CpG as an affordable and accessible vaccine.

Among various AH:PRR agonist formulations, AH:CpG elicited the highest immune responses in both young and aged mice. We observed that vaccine immune responses were generally lower in aged mice than in young adult mice, even in the group receiving RBD formulated with AH:CpG. While the lower levels of anti-RBD Abs observed in aged mice are likely sufficient for protection, we found that an additional booster dose in the aged overcame the observed age-dependent reductions in vaccine response and protected aged mice from SARS-CoV-2 challenge. We employed AH, which has been used for >90 years with a firmly established record of safety and efficacy (*32*) and AS01B, which recently demonstrated excellent adjuvant effects among elderly humans (*33, 34*), as "benchmarking" adjuvants to compare the exploratory adjuvanted formulations with more established adjuvants. In this context, we demonstrated that the AH:CpG adjuvanted vaccine was superior to a vaccine adjuvanted only with AH and was non-inferior to AS01B. In the context of the aged mice prime-boost setting, AH:CpG-adjuvanted SARS-CoV-2 RBD significantly outperformed AS01B with respect to functional anti-RBD inhibition (Geometric mean (GM) with SD, 57±2% *vs*. 14±3%) and neutralizing Abs titers (2344 ± 7 *vs.* 117± 4).

In this study, AH:CpG dramatically enhanced vaccine immune responses compared to vaccines adjuvanted with AH or CpG alone in both young and aged mice. AH:PRR agonist formulations have shown promising adjuvanticity in preclinical models, and AS04 (a formulation of aluminum salts and MPLA) is employed in several licensed vaccines (*32*). While the precise mechanism of action of AH:PRR agonist formulations has not been completely uncovered and is potentially influenced by the degree of adsorption of PRR ligands onto AH, the effects of these formulations are at least in part mediated by enhanced activation of innate immune cells at the

297 injection site (*31, 55*). In our murine model, we also show that AH:CpG and CpG alone induce
298 comparable proinflammatory gene expression profiles in dLNs. To gain additional mechanistic
299 insight and increase the translational relevance of our findings, we tested the activity of AH:CpG
300 on human PBMCs isolated from young adults and older individuals and found that this adjuvant
301 formulation synergistically enhances cytokine and chemokine production compared to AH or
302 CpG. These results might be explained by either 1) synergistic activation by AH and CpG of
303 distinct molecular pathways, and/or 2) adsorption of CpG onto AH leading to the formation of
304 macromolecular complexes that are more efficiently internalized and/or lead to enhanced TLR9
305 activation. Further work is required to define the underlying molecular mechanism of action of
306 AH:CpG *in vivo* and *in vitro*.
307
308 The rationale for use of a synthetic TLR9 agonist CpG as an adjuvant for SARS-CoV-2 subunit
309 vaccine is multi-fold. First, CpG has been used as a vaccine adjuvant in licensed vaccines with
310 well-known mechanisms, substantial safety data, and confirmed effectiveness (*56, 57*). Second,
311 CpG has demonstrated adjuvant effects in elderly populations. CpG enhanced vaccinal antigen
312 immunogenicity in aged mouse and porcine models (*58-63*). Several human trials demonstrated
313 that older individuals had a higher seroprotection rate when immunized with the CpG-adjuvanted
314 hepatitis B vaccine compared to the conventional alum-adjuvanted vaccine (*64, 65*). Finally,
315 AH:CpG-adjuvanted SARS-CoV-2 Spike vaccines have demonstrated safety, immunogenicity,
316 and efficacy in several young adult animal models (*51, 66, 67*), and in a human clinical study
317 involving an older population (*12*). Furthermore, Biological E has recently completed early
318 phase (1 and 2) trials of a AH:CpG-adjuvanted SARS-CoV-2 RBD protein vaccine (trial #
319 CTRI/2020/11/029032) which was intended for low- and middle-income countries, and are

currently advancing through manufacturing and clinical development through a large-scale phase 3 trial in India (*17*). CpG is classified into 4 major classes, with distinct activation profiles of human cells (*68*). Class B CpG-1018 has been extensively evaluated in clinical trials. We observed that CpG-1018 and the class C CpG-2395 formulated with AH elicit comparable levels of neutralizing Abs, resulting in adjuvanted RBD formulations that were both non-inferior to the clinical-grade BNT162b2 Spike mRNA vaccine. Studies of TLR7/8 agonists as precision adjuvants with robust activity in early life (*69*), including in enhancing Spike immunogenicity in the young (*70*), further support the use of adjuvants to enhance vaccine immunogenicity in target populations. Together, and in light of our results in the older individuals, these studies suggest that precision adjuvant approaches hold substantial promise to generate scalable adjuvanted SARS-CoV-2 vaccine formulations that do not require freezing and afford robust protection to vulnerable populations across the lifespan.

Our study features several strengths, including (a) defining a combination adjuvantation system based on the common AH backbone that demonstrated mathematical synergy in its ability to activate human mononuclear cells; (b) accounting for age-specific immunity that can play major roles in vaccine immunogenicity and is often overlooked in vaccine discovery; (c) accounting for species-specificity by assessing the activity of the adjuvant formulation in human PBMCs *in vitro* and in mice *in vivo*; (d) testing the ability of the adjuvanted formulation to protect in a SARS-CoV-2 challenge model; and (e) benchmarking to the authorized BNT162b2 Spike mRNA vaccine to place our studies in context. As with any research our study also has some limitations, including that (a) we performed *in vivo* analysis only in mice, establishing the need for future translational research in additional animal models and humans and (b) all

adjuvants/antigens were compared in single dose and further analysis should be performed in multiple doses to evaluate both efficacy and reactogenicity. Nevertheless, since we used standard doses of adjuvants/antigens in mouse systems (e.g., 1/30 and 1/18th of the human dose for CpG (*12*) and BNT162b2 (*3*) respectively, to compare the CpG-adjuvanted RBD subunit vaccine to the mRNA vaccine), it should be underscored that the results in this study hold promising value from a translational perspective.

Recently, several SARS-CoV-2 variants of concern have emerged harboring mutations in the RBD region and showing various degrees of reduced neutralization by serum samples obtained from convalescent or vaccinated individuals (*38-40*). It is likely that booster doses that account for mutations in the Spike protein will be required in order to achieve complete immunity against such variants (*71*). Several vaccines composed of multiple protein antigens adsorbed onto aluminum salts alone or co-formulated with MPLA have been produced (*55, 72*). We speculate that an AH:CpG-adjuvanted coronavirus vaccine formulation incorporating RBD proteins from different SARS-CoV-2 strains (and potentially other coronaviruses) may promote cross-strain protective immunity.

Overall, the current study aimed to evaluate an optimal adjuvant formulation to improve the protective response of RBD-based subunit vaccines in the elderly population, which is otherwise reduced as an effect of aging. We show that an AH:CpG adjuvant formulation induces potent anti-RBD responses in both young and aged mice and overcomes both the poor immunogenicity of the antigen and impaired immune responses in the aged. We discovered unique immunological properties of the AH:CpG adjuvant formulation that demonstrated synergistic

366 enhancement of the production of multiple cytokines and chemokines from human adult and
367 elderly PBMCs *in vitro*. These data indicate that formulating RBD with AH:CpG represents a
368 promising approach to develop a practical (e.g., not requiring low temperature storage), scalable,
369 effective, and affordable vaccine that may be effective across multiple age groups and could
370 potentially incorporate multiple RBD proteins to achieve cross-strain protection.
371

MATERIALS AND METHODS

Study design. The aim of this study was to assess optimal combinations of RBD antigen and adjuvants in pre-clinical models that take age-dependent vaccine immune responses and COVID-19 susceptibility into account. To this end, we used age-specific mouse *in vivo* and human *in vitro* models. Sample size and age criteria was chosen empirically based on results of previous studies. Mouse experiments aimed to include in total 10 mice per group and were combined from two individual experiments. Mice were randomly assigned to different treatment groups. In order to assess the translational relevance and potential mechanism of an adjuvant formulation, we designed human *in vitro* study with peripheral blood collected from healthy young adults, aged 18–40 y (n = 6), and older participants, aged ≥ 65 years (n = 6), with approval from the Ethics Committee of the Boston Children's Hospital (protocol number X07-05-0223) and Institutional Review Board of Brigham and Women's Hospital, Boston (protocol number 2013P002473). All participants signed an informed consent form prior to enrollment. Investigators were not blinded. No data outliers were excluded.

Animals. Female, 3 months old BALB/c mice were purchased from Jackson Laboratory (Bar Harbor, ME). Female, 12-13 months old BALB/c mice purchased from Taconic Biosciences (Germantown, NY) were used for aged mice experiments. Mice were housed under specific pathogen-free conditions at Boston Children's Hospital, and all the procedures were approved under the Institutional Animal Care and Use Committee (IACUC) and operated under the supervision of the Department of Animal Resources at Children's Hospital (ARCH) (Protocol number 19-02-3897R). At the University of Maryland School of Medicine, mice were housed in

a biosafety level 3 (BSL3) facility for all SARS-CoV-2 infections with all the procedures approved under the IACUC (Protocol number #1120004) to MBF.

SARS-CoV-2 Spike and RBD expression and purification. Full length SARS-CoV-2 Spike glycoprotein (M1-Q1208, GenBank MN90894) and RBD constructs (amino acid residues R319-K529, GenBank MN975262.1), both with an HRV3C protease cleavage site, a TwinStrepTag and an 8XHisTag at C-terminus were obtained from Barney S. Graham (NIH Vaccine Research Center) and Aaron G. Schmidt (Ragon Institute), respectively. These mammalian expression vectors were used to transfect Expi293F suspension cells (Thermo Fisher) using polyethylenimine (Polysciences). Cells were allowed to grow in 37°C, 8% CO_2 for additional 5 days before harvesting for purification. Protein was purified in a PBS buffer (pH 7.4) from filtered supernatants by using either StrepTactin resin (IBA) or Cobalt-TALON resin (Takara). Affinity tags were cleaved off from eluted protein samples by HRV 3C protease, and tag removed proteins were further purified by size-exclusion chromatography using a Superose 6 10/300 column (Cytiva) for full length Spike and a Superdex 75 10/300 Increase column (Cytiva) for RBD domain in a PBS buffer (pH 7.4).

Adjuvants and immunization. The adjuvants and their doses used were: Alhydrogel adjuvant 2% (100 µg), 2'3'-cGAMP (10 µg), Poly (I:C) HMW (50 µg), CpG-ODN 2395 (50 µg), AddaS03 (25 µL) (all from InvivoGen, San Diego, CA), CpG-ODN 1018 (50 µg, 5' TGA CTG TGA ACG TTC GAG ATG A 3') (Integrated DNA Technologies, Coralville, IA), PHAD (50 µg) (Avanti Polar Lipids, Alabaster, AL), and AS01B (40 µL) (obtained from the Shingrix vaccine, GSK Biologicals SA, Belgium). Mice were injected with 10 µg of recombinant

monomeric SARS-CoV-2 RBD protein, with or without adjuvants. Each PRR agonist was formulated with and without aluminum hydroxide. Mock treatment mice received phosphate-buffered saline (PBS) alone. BNT162b2 Spike mRNA vaccine (Pfizer-BioNTech) was obtained as residual volumes in used vials from the Boston Children's Hospital employee vaccine clinic, strictly using material that would only otherwise be discarded, and was used within 6 hours from the time of reconstitution. BNT162b2 suspension (100 µg/mL) was diluted 1:3 in PBS, and 50 µL (1.67 µg) was injected. Injections (50 µL) were administered intramuscularly in the caudal thigh on Days -0, -14 (both age groups), and Day 28 (aged mice only, where relevant). Blood samples were collected 2 weeks post-immunization.

ELISA. RBD- and Spike-specific antibody levels were quantified in serum samples by ELISA by modification of a previously described protocol(*73*). Briefly, high-binding flat-bottom 96-well plates (Corning, NY) were coated with 50 ng/well RBD or 25 ng/well Spike and incubated overnight at 4 °C. Plates were washed with 0.05% Tween 20 PBS and blocked with 1% BSA PBS for 1 h at room temperature (RT). Serum samples were serially diluted 4-fold from 1:100 up to 1:1.05E8 and then incubated for 2 hours at RT. Plates were washed three times and incubated for 1 hour at RT with HRP-conjugated anti-mouse IgG, IgG1, IgG2a, or IgG2c (Southern Biotech). Plates were washed five times and developed with tetramethylbenzidine (1-Step Ultra TMB-ELISA Substrate Solution, ThermoFisher, for RBD-ELISA, and BD OptEIA Substrate Solution, BD Biosciences, for Spike ELISA) for 5 min, then stopped with 2 N H_2SO_4. Optical densities (ODs) were read at 450 nm with SpectraMax iD3 microplate reader (Molecular Devices). End-point titers were calculated as the dilution that emitted an optical density

exceeding a 3× background. An arbitrary value of 50 was assigned to the samples with OD values below the limit of detection for which it was not possible to interpolate the titer.

hACE2/RBD inhibition assay. The hACE2/RBD inhibition assay employed a modification of a previously published protocol(*74*). Briefly, high-binding flat-bottom 96-well plates (Corning, NY) were coated with 100 ng/well recombinant human ACE2 (hACE2) (Sigma-Aldrich) in PBS, incubated overnight at 4°C, washed three times with 0.05% Tween 20 PBS, and blocked with 1% BSA PBS for 1 hour at RT. Each serum sample was diluted 1:160, pre-incubated with 3 ng of RBD-Fc in 1% BSA PBS for 1 hour at RT, and then transferred to the hACE2-coated plate. RBD-Fc without pre-incubation with serum samples was added as a positive control, and 1% BSA PBS without serum pre-incubation was added as a negative control. Plates were then washed three times and incubated with HRP-conjugated anti-human IgG Fc (Southern Biotech) for 1 hour at RT. Plates were washed five times and developed with tetramethylbenzidine (BD OptEIA Substrate Solution, BD Biosciences) for 5 min, then stopped with 2 N H_2SO_4. The optical density was read at 450 nm with SpectraMax iD3 microplate reader (Molecular Devices). Percentage inhibition of RBD binding to hACE2 was calculated with the following formula: Inhibition (%) = [1 – (Sample OD value – Negative Control OD value)/(Positive Control OD value – Negative Control OD value)] x 100.

SARS-CoV-2 neutralization titer determination. All serum samples were heat-inactivated at 56°C for 30 min to remove complement and allowed to equilibrate to RT prior to processing for neutralization titer. Samples were diluted in duplicate to an initial dilution of 1:5 or 1:10 followed by 1:2 serial dilutions (vaccinated sample), resulting in a 12-dilution series with each

462 well containing 100 µL. All dilutions were performed in DMEM (Quality Biological),
463 supplemented with 10% (v/v) fetal bovine serum (heat-inactivated, Sigma), 1% (v/v)
464 penicillin/streptomycin (Gemini Bio-products) and 1% (v/v) L-glutamine (2 mM final
465 concentration, Gibco). Dilution plates were then transported into the BSL-3 laboratory and 100
466 µL of diluted SARS-CoV-2 (WA-1, courtesy of Dr. Natalie Thornburg/CDC) inoculum was
467 added to each well to result in a multiplicity of infection (MOI) of 0.01 upon transfer to titering
468 plates. A non-treated, virus-only control and mock infection control were included on every plate.
469 The sample/virus mixture was then incubated at 37°C (5.0% CO_2) for 1 hour before transferring
470 to 96-well titer plates with confluent VeroE6 cells. Titer plates were incubated at 37°C (5.0%
471 CO_2) for 72 hours, followed by CPE determination for each well in the plate. The first sample
472 dilution to show CPE was reported as the minimum sample dilution required to neutralize >99%
473 of the concentration of SARS-CoV-2 tested (NT99).
474
475 **Pseudovirus neutralization assay.** The SARS-CoV-2 pseudoviruses expressing a luciferase
476 reporter gene were generated in an approach similar to as described previously (*75, 76*). Briefly,
477 the packaging plasmid psPAX2 (AIDS Resource and Reagent Program), luciferase reporter
478 plasmid pLenti-CMV Puro-Luc (Addgene), and spike protein expressing pcDNA3.1-SARS
479 CoV-2 SΔCT of variants were co-transfected into HEK293T cells by lipofectamine 2000
480 (ThermoFisher). Pseudoviruses of SARS-CoV-2 variants were generated by using WA1/2020
481 strain (Wuhan/WIV04/2019, GISAID accession ID: EPI_ISL_402124), B.1.1.7 variant (GISAID
482 accession ID: EPI_ISL_601443), or B.1.351 variant (GISAID accession ID: EPI_ISL_712096).
483 The supernatants containing the pseudotype viruses were collected 48 h post-transfection, which
484 were purified by centrifugation and filtration with 0.45 µm filter. To determine the neutralization

activity of the plasma or serum samples from participants, HEK293T-hACE2 cells were seeded in 96-well tissue culture plates at a density of 1.75 x 10^4 cells/well overnight. Three-fold serial dilutions of heat inactivated serum or plasma samples were prepared and mixed with 50 µL of pseudovirus. The mixture was incubated at 37°C for 1 h before adding to HEK293T-hACE2 cells. 48 h after infection, cells were lysed in Steady-Glo Luciferase Assay (Promega) according to the manufacturer's instructions. SARS-CoV-2 neutralization titers were defined as the sample dilution at which a 50% reduction in relative light unit (RLU) was observed relative to the average of the virus control wells.

Splenocyte restimulation assay. Immunized mice were sacrificed 2 weeks after the final immunization, and spleens were collected. To isolate splenocytes, spleens were mashed through a 70 µm cell strainer, and the resulting cell suspensions were washed with PBS and incubated with 2 mL of ACK lysis buffer (Gibco) for 2 minutes at RT to lyse erythrocytes. Splenocytes were washed again with PBS and plated in flat-bottom 96-well plates (2 x 10^6 cells per well). Then, SARS-CoV-2 Spike peptides (PepTivator SARS-CoV-2 Prot_S, Miltenyi Biotec) were added at a final concentration of 0.6 nmol/ml in the presence of 1 µg/mL anti-CD28 antibody (total cell culture volume, 200 µL per well). After 24 (for IL-2 and IL-4) and 96 (for IFNγ) hours, supernatants were harvested, and cytokine levels were measured by ELISA (Invitrogen) according to the manufacturer's protocol.

SARS-CoV-2 mouse challenge study. Mice were anesthetized by intraperitoneal injection 50 µL of a mix of xylazine (0.38 mg/mouse) and ketamine (1.3 mg/mouse) diluted in PBS. Mice were then intranasally inoculated with 1 x 10^3 PFU of mouse-adapted SARS-CoV-2 (MA10,

courtesy of Dr. Ralph Baric (UNC)) in 50 µL divided between nares(*35*). Different doses of SARS-CoV-2 were used where indicated. Challenged mice were weighed on the day of infection and daily for up to 4 days post-infection. At 4-day post-infection, mice were sacrificed, and lungs were harvested to determine virus titer by a plaque assay and prepared for histological scoring.

SARS-CoV-2 plaque assay. SARS-CoV-2 lung titers were quantified by homogenizing harvested lungs in PBS (Quality Biological Inc.) using 1.0 mm glass beads (Sigma Aldrich) and a Beadruptor (Omni International Inc.). Homogenates were added to Vero E6 cells and SARS-CoV-2 virus titers determined by counting plaque-forming units (pfu) using a 6-point dilution curve.

Histopathology analysis. Slides were prepared as 5-µm sections and stained with hematoxylin and eosin. A pathologist was blinded to information identifying the treatment groups and fields were examined by light microscopy and analyzed. The severity of interstitial inflammation was evaluated and converted to a score of 0-4 with 0 being no inflammation and 4 being most severe. Interstitial inflammation was evaluated for the number of neutrophils present in the interstitial space as well as the extent of neutrophilic apoptosis. Once scoring was complete, scores for each group were averaged and the standard deviation for the scoring was computed.

Mouse *in vivo* LNs gene expression analysis by quantitative real-time PCR array. Mice were subcutaneously injected on Day 0 with the indicated treatments in a volume of 50 µL on each side of the back (one side for the compound and the contralateral side for saline of vehicle control). Twenty-four hours post-injection, draining (brachial) LNs were collected for

subsequent analysis. LNs were transferred to a beadbeater and homogenized in TRI Reagent (Zymo Research). Samples were then centrifuged, and the clear supernatant was transferred to a new tube for subsequent RNA isolation. RNA was isolated from TRI Reagent samples using phenol-chloroform extraction or column-based extraction systems (Direct-zol RNA Miniprep, Zymo Research) according to the manufacturer's protocol. RNA concentration and purity (260/280 and 260/230 ratios) were measured by NanoDrop (ThermoFisher Scientific). cDNA was prepared from RNA with RT^2 First Strand Kit, according to the manufacturer's instructions (Qiagen). cDNA was quantified using 96-well PCR array analysis on a PAMM-150ZA plate (Cytokines & Chemokines) and PAMM-016ZA plate (Type I Interferon Response) (both Qiagen). Quantitative real time-PCR (QRT-PCR) was run on a 7300 real-time PCR system (Applied Biosystems – Life Technologies, Carlsbad, CA). mRNA levels were normalized to 3 housekeeping genes: *Actb*, *Gapdh*, and *Gusb*. Relative quantification of gene expression was calculated by the $\Delta\Delta Ct$ (relative expression over PBS treatment group).

Human PBMC isolation. PBMCs were isolated based previously described protocols (*77*). Briefly, heparinized whole blood was centrifuged at 500 g for 10 min, then the upper layer of platelet-rich plasma was removed. Plasma was centrifuged at 3000 g for 10 min, and platelet-poor plasma (PPP) was collected and stored on ice. The remaining blood was reconstituted to its original volume with heparinized DPBS and layered on Ficoll-Paque gradients (Cytiva) in Accuspin tubes (Sigma-Aldrich). PBMCs were collected after centrifugation and washed twice with PBS.

553 **Human PBMCs stimulation.** PBMCs were resuspended at a concentration of 200,000 cells per
554 well in a 96-well U-bottom plate (Corning) in 200 µL RPMI 1640 media (Gibco) supplemented
555 with 10% autologous PPP, 100 IU/mL penicillin, 100 µg/mL streptomycin, and 2 mM L-
556 glutamine. PBMCs were incubated for 24 hrs at 37ºC in a humidified incubator at 5% CO_2 with
557 indicated treatments. After culture, plates were centrifuged at 500 g and supernatants were
558 removed by pipetting without disturbing the cell pellet. Cytokine expression profiles in cell
559 culture supernatants were measured using customized Milliplex human cytokine magnetic bead
560 panels (Milliplex). Assays were analyzed on the Luminex FLEXMAP 3D employing xPONENT
561 software (Luminex) and Millipore Milliplex Analyst. Cytokine measurements were excluded
562 from analysis if fewer than 30 beads were recovered. Synergy was evaluated using the Loewe
563 definition of additivity, with D > 1 indicating antagonism, D = 1 additivity, and D < 1 synergy
564 (*78*). In order to fit regression curves more closely to the data, higher concentrations were
565 excluded from linear regressions when calculating D values if the cytokine levels plateaued or
566 decreased.
567
568 **Statistical analysis.** Statistical analyses were performed using Prism v9.0.2 (GraphPad
569 Software) and R software environment v4.0.4. *P* values < 0.05 were considered significant. Data
570 were analyzed by one- or two-way ANOVAs followed by post-hoc Tukey's test or Dunnett's test
571 for multiple comparisons. Non-normally distributed data were log-transformed. In the animal
572 experiences, time to event were analyzed using Kaplan-Meier estimates and compared across
573 groups using the Log-rank test. For human in vitro PBMC assay, unpaired Mann-Whitney tests
574 were applied at each concentration. We conducted gene expression analyses with R 4.0.4 using
575 packages 'ggplot2', 'dplyr', and 'MASS' for the transcript abundance determination of gene

576 arrays in each group. We log-transformed data before performing principal component analysis
577 (PCA) and unsupervised hierarchical clustering using R packages 'prcomp' and 'pheatmap'
578 respectively. We analyzed the differential gene expression using generalized linear models
579 (GLMs) with treatment and age as fixed effects. We then enriched the differentially expressed
580 genes using the blood transcriptional module method based on an existing protocol (Li et al.,
581 2013- PMC: 24336226).
582

583 **REFERENCES**

584 1. W. C. Koff, T. Schenkelberg, T. Williams, R. S. Baric, A. McDermott, C. M. Cameron,
585 M. J. Cameron, M. B. Friemann, G. Neumann, Y. Kawaoka, A. A. Kelvin, T. M. Ross, S.
586 Schultz-Cherry, T. D. Mastro, F. H. Priddy, K. A. Moore, J. T. Ostrowsky, M. T.
587 Osterholm, J. Goudsmit, Development and deployment of COVID-19 vaccines for those
588 most vulnerable. *Science Translational Medicine* **13**, eabd1525 (2021).
589 2. L. R. Baden, H. M. El Sahly, B. Essink, K. Kotloff, S. Frey, R. Novak, D. Diemert, S. A.
590 Spector, N. Rouphael, C. B. Creech, J. McGettigan, S. Kehtan, N. Segall, J. Solis, A.
591 Brosz, C. Fierro, H. Schwartz, K. Neuzil, L. Corey, P. Gilbert, H. Janes, D. Follmann, M.
592 Marovich, J. Mascola, L. Polakowski, J. Ledgerwood, B. S. Graham, H. Bennett, R.
593 Pajon, C. Knightly, B. Leav, W. Deng, H. Zhou, S. Han, M. Ivarsson, J. Miller, T. Zaks,
594 Efficacy and Safety of the mRNA-1273 SARS-CoV-2 Vaccine. *The New England*
595 *journal of medicine*, (2020).
596 3. F. P. Polack, S. J. Thomas, N. Kitchin, J. Absalon, A. Gurtman, S. Lockhart, J. L. Perez,
597 G. Pérez Marc, E. D. Moreira, C. Zerbini, R. Bailey, K. A. Swanson, S. Roychoudhury,
598 K. Koury, P. Li, W. V. Kalina, D. Cooper, R. W. Frenck, Jr., L. L. Hammitt, Ö. Türeci, H.
599 Nell, A. Schaefer, S. Ünal, D. B. Tresnan, S. Mather, P. R. Dormitzer, U. Şahin, K. U.
600 Jansen, W. C. Gruber, Safety and Efficacy of the BNT162b2 mRNA Covid-19 Vaccine.
601 *The New England journal of medicine* **383**, 2603-2615 (2020).
602 4. J. Sadoff, M. Le Gars, G. Shukarev, D. Heerwegh, C. Truyers, A. M. de Groot, J. Stoop,
603 S. Tete, W. Van Damme, I. Leroux-Roels, P. J. Berghmans, M. Kimmel, P. Van Damme,
604 J. de Hoon, W. Smith, K. E. Stephenson, S. C. De Rosa, K. W. Cohen, M. J. McElrath, E.
605 Cormier, G. Scheper, D. H. Barouch, J. Hendriks, F. Struyf, M. Douoguih, J. Van Hoof,

H. Schuitemaker, Interim Results of a Phase 1-2a Trial of Ad26.COV2.S Covid-19 Vaccine. *The New England journal of medicine*, (2021).

5. K. S. Corbett, D. K. Edwards, S. R. Leist, O. M. Abiona, S. Boyoglu-Barnum, R. A. Gillespie, S. Himansu, A. Schäfer, C. T. Ziwawo, A. T. DiPiazza, K. H. Dinnon, S. M. Elbashir, C. A. Shaw, A. Woods, E. J. Fritch, D. R. Martinez, K. W. Bock, M. Minai, B. M. Nagata, G. B. Hutchinson, K. Wu, C. Henry, K. Bahl, D. Garcia-Dominguez, L. Ma, I. Renzi, W. P. Kong, S. D. Schmidt, L. Wang, Y. Zhang, E. Phung, L. A. Chang, R. J. Loomis, N. E. Altaras, E. Narayanan, M. Metkar, V. Presnyak, C. Liu, M. K. Louder, W. Shi, K. Leung, E. S. Yang, A. West, K. L. Gully, L. J. Stevens, N. Wang, D. Wrapp, N. A. Doria-Rose, G. Stewart-Jones, H. Bennett, G. S. Alvarado, M. C. Nason, T. J. Ruckwardt, J. S. McLellan, M. R. Denison, J. D. Chappell, I. N. Moore, K. M. Morabito, J. R. Mascola, R. S. Baric, A. Carfi, B. S. Graham, SARS-CoV-2 mRNA vaccine design enabled by prototype pathogen preparedness. *Nature* **586**, 567-571 (2020).

6. K. S. Corbett, B. Flynn, K. E. Foulds, J. R. Francica, S. Boyoglu-Barnum, A. P. Werner, B. Flach, S. O'Connell, K. W. Bock, M. Minai, B. M. Nagata, H. Andersen, D. R. Martinez, A. T. Noe, N. Douek, M. M. Donaldson, N. N. Nji, G. S. Alvarado, D. K. Edwards, D. R. Flebbe, E. Lamb, N. A. Doria-Rose, B. C. Lin, M. K. Louder, S. O'Dell, S. D. Schmidt, E. Phung, L. A. Chang, C. Yap, J. M. Todd, L. Pessaint, A. Van Ry, S. Browne, J. Greenhouse, T. Putman-Taylor, A. Strasbaugh, T. A. Campbell, A. Cook, A. Dodson, K. Steingrebe, W. Shi, Y. Zhang, O. M. Abiona, L. Wang, A. Pegu, E. S. Yang, K. Leung, T. Zhou, I. T. Teng, A. Widge, I. Gordon, L. Novik, R. A. Gillespie, R. J. Loomis, J. I. Moliva, G. Stewart-Jones, S. Himansu, W. P. Kong, M. C. Nason, K. M. Morabito, T. J. Ruckwardt, J. E. Ledgerwood, M. R. Gaudinski, P. D. Kwong, J. R.

Mascola, A. Carfi, M. G. Lewis, R. S. Baric, A. McDermott, I. N. Moore, N. J. Sullivan, M. Roederer, R. A. Seder, B. S. Graham, Evaluation of the mRNA-1273 Vaccine against SARS-CoV-2 in Nonhuman Primates. *The New England journal of medicine* **383**, 1544-1555 (2020).

7. A. B. Vogel, I. Kanevsky, Y. Che, K. A. Swanson, A. Muik, M. Vormehr, L. M. Kranz, K. C. Walzer, S. Hein, A. Güler, J. Loschko, M. S. Maddur, A. Ota-Setlik, K. Tompkins, J. Cole, B. G. Lui, T. Ziegenhals, A. Plaschke, D. Eisel, S. C. Dany, S. Fesser, S. Erbar, F. Bates, D. Schneider, B. Jesionek, B. Sänger, A. K. Wallisch, Y. Feuchter, H. Junginger, S. A. Krumm, A. P. Heinen, P. Adams-Quack, J. Schlereth, S. Schille, C. Kröner, R. de la Caridad Güimil Garcia, T. Hiller, L. Fischer, R. S. Sellers, S. Choudhary, O. Gonzalez, F. Vascotto, M. R. Gutman, J. A. Fontenot, S. Hall-Ursone, K. Brasky, M. C. Griffor, S. Han, A. A. H. Su, J. A. Lees, N. L. Nedoma, E. H. Mashalidis, P. V. Sahasrabudhe, C. Y. Tan, D. Pavliakova, G. Singh, C. Fontes-Garfias, M. Pride, I. L. Scully, T. Ciolino, J. Obregon, M. Gazi, R. Carrion, Jr., K. J. Alfson, W. V. Kalina, D. Kaushal, P. Y. Shi, T. Klamp, C. Rosenbaum, A. N. Kuhn, Ö. Türeci, P. R. Dormitzer, K. U. Jansen, U. Sahin, BNT162b vaccines protect rhesus macaques from SARS-CoV-2. *Nature* **592**, 283-289 (2021).

8. N. B. Mercado, R. Zahn, F. Wegmann, C. Loos, A. Chandrashekar, J. Yu, J. Liu, L. Peter, K. McMahan, L. H. Tostanoski, X. He, D. R. Martinez, L. Rutten, R. Bos, D. van Manen, J. Vellinga, J. Custers, J. P. Langedijk, T. Kwaks, M. J. G. Bakkers, D. Zuijdgeest, S. K. Rosendahl Huber, C. Atyeo, S. Fischinger, J. S. Burke, J. Feldman, B. M. Hauser, T. M. Caradonna, E. A. Bondzie, G. Dagotto, M. S. Gebre, E. Hoffman, C. Jacob-Dolan, M. Kirilova, Z. Li, Z. Lin, S. H. Mahrokhian, L. F. Maxfield, F. Nampanya, R. Nityanandam,

J. P. Nkolola, S. Patel, J. D. Ventura, K. Verrington, H. Wan, L. Pessaint, A. Van Ry, K. Blade, A. Strasbaugh, M. Cabus, R. Brown, A. Cook, S. Zouantchangadou, E. Teow, H. Andersen, M. G. Lewis, Y. Cai, B. Chen, A. G. Schmidt, R. K. Reeves, R. S. Baric, D. A. Lauffenburger, G. Alter, P. Stoffels, M. Mammen, J. Van Hoof, H. Schuitemaker, D. H. Barouch, Single-shot Ad26 vaccine protects against SARS-CoV-2 in rhesus macaques. *Nature* **586**, 583-588 (2020).

9. M. S. Gebre, L. A. Brito, L. H. Tostanoski, D. K. Edwards, A. Carfi, D. H. Barouch, Novel approaches for vaccine development. *Cell* **184**, 1589-1603 (2021).

10. I. T. Katz, R. Weintraub, L. G. Bekker, A. M. Brandt, From Vaccine Nationalism to Vaccine Equity - Finding a Path Forward. *The New England journal of medicine* **384**, 1281-1283 (2021).

11. C. Keech, G. Albert, I. Cho, A. Robertson, P. Reed, S. Neal, J. S. Plested, M. Zhu, S. Cloney-Clark, H. Zhou, G. Smith, N. Patel, M. B. Frieman, R. E. Haupt, J. Logue, M. McGrath, S. Weston, P. A. Piedra, C. Desai, K. Callahan, M. Lewis, P. Price-Abbott, N. Formica, V. Shinde, L. Fries, J. D. Lickliter, P. Griffin, B. Wilkinson, G. M. Glenn, Phase 1-2 Trial of a SARS-CoV-2 Recombinant Spike Protein Nanoparticle Vaccine. *The New England journal of medicine* **383**, 2320-2332 (2020).

12. P. Richmond, L. Hatchuel, M. Dong, B. Ma, B. Hu, I. Smolenov, P. Li, P. Liang, H. H. Han, J. Liang, R. Clemens, Safety and immunogenicity of S-Trimer (SCB-2019), a protein subunit vaccine candidate for COVID-19 in healthy adults: a phase 1, randomised, double-blind, placebo-controlled trial. *Lancet (London, England)*, (2021).

13. S. Xia, Y. Zhang, Y. Wang, H. Wang, Y. Yang, G. F. Gao, W. Tan, G. Wu, M. Xu, Z. Lou, W. Huang, W. Xu, B. Huang, H. Wang, W. Wang, W. Zhang, N. Li, Z. Xie, L. Ding,

W. You, Y. Zhao, X. Yang, Y. Liu, Q. Wang, L. Huang, Y. Yang, G. Xu, B. Luo, W. Wang, P. Liu, W. Guo, X. Yang, Safety and immunogenicity of an inactivated SARS-CoV-2 vaccine, BBIBP-CorV: a randomised, double-blind, placebo-controlled, phase 1/2 trial. *Lancet Infect Dis* **21**, 39-51 (2021).

14. Y. Zhang, G. Zeng, H. Pan, C. Li, Y. Hu, K. Chu, W. Han, Z. Chen, R. Tang, W. Yin, X. Chen, Y. Hu, X. Liu, C. Jiang, J. Li, M. Yang, Y. Song, X. Wang, Q. Gao, F. Zhu, Safety, tolerability, and immunogenicity of an inactivated SARS-CoV-2 vaccine in healthy adults aged 18-59 years: a randomised, double-blind, placebo-controlled, phase 1/2 clinical trial. *Lancet Infect Dis* **21**, 181-192 (2021).

15. N. C. Kyriakidis, A. López-Cortés, E. V. González, A. B. Grimaldos, E. O. Prado, SARS-CoV-2 vaccines strategies: a comprehensive review of phase 3 candidates. *NPJ vaccines* **6**, 28 (2021).

16. CTRI. Biological E's novel Covid-19 vaccine of SARS-CoV-2 for protection against Covid-19 disease., <http://ctri.nic.in/Clinicaltrials/pmaindet2.php?trialid=48329&EncHid=&userName=covid-19%20vaccine> Accessed May 1, 2021

17. The New York Times. Coronavirus Vaccine Tracker, <https://www.nytimes.com/interactive/2020/science/coronavirus-vaccine-tracker.html>, Accessed May 3, 2021

18. J. Yang, W. Wang, Z. Chen, S. Lu, F. Yang, Z. Bi, L. Bao, F. Mo, X. Li, Y. Huang, W. Hong, Y. Yang, Y. Zhao, F. Ye, S. Lin, W. Deng, H. Chen, H. Lei, Z. Zhang, M. Luo, H. Gao, Y. Zheng, Y. Gong, X. Jiang, Y. Xu, Q. Lv, D. Li, M. Wang, F. Li, S. Wang, G. Wang, P. Yu, Y. Qu, L. Yang, H. Deng, A. Tong, J. Li, Z. Wang, J. Yang, G. Shen, Z.

Zhao, Y. Li, J. Luo, H. Liu, W. Yu, M. Yang, J. Xu, J. Wang, H. Li, H. Wang, D. Kuang, P. Lin, Z. Hu, W. Guo, W. Cheng, Y. He, X. Song, C. Chen, Z. Xue, S. Yao, L. Chen, X. Ma, S. Chen, M. Gou, W. Huang, Y. Wang, C. Fan, Z. Tian, M. Shi, F. S. Wang, L. Dai, M. Wu, G. Li, G. Wang, Y. Peng, Z. Qian, C. Huang, J. Y. Lau, Z. Yang, Y. Wei, X. Cen, X. Peng, C. Qin, K. Zhang, G. Lu, X. Wei, A vaccine targeting the RBD of the S protein of SARS-CoV-2 induces protective immunity. *Nature* **586**, 572-577 (2020).

19. L. Piccoli, Y. J. Park, M. A. Tortorici, N. Czudnochowski, A. C. Walls, M. Beltramello, C. Silacci-Fregni, D. Pinto, L. E. Rosen, J. E. Bowen, O. J. Acton, S. Jaconi, B. Guarino, A. Minola, F. Zatta, N. Sprugasci, J. Bassi, A. Peter, A. De Marco, J. C. Nix, F. Mele, S. Jovic, B. F. Rodriguez, S. V. Gupta, F. Jin, G. Piumatti, G. Lo Presti, A. F. Pellanda, M. Biggiogero, M. Tarkowski, M. S. Pizzuto, E. Cameroni, C. Havenar-Daughton, M. Smithey, D. Hong, V. Lepori, E. Albanese, A. Ceschi, E. Bernasconi, L. Elzi, P. Ferrari, C. Garzoni, A. Riva, G. Snell, F. Sallusto, K. Fink, H. W. Virgin, A. Lanzavecchia, D. Corti, D. Veesler, Mapping Neutralizing and Immunodominant Sites on the SARS-CoV-2 Spike Receptor-Binding Domain by Structure-Guided High-Resolution Serology. *Cell* **183**, 1024-1042.e1021 (2020).

20. L. Premkumar, B. Segovia-Chumbez, R. Jadi, D. R. Martinez, R. Raut, A. Markmann, C. Cornaby, L. Bartelt, S. Weiss, Y. Park, C. E. Edwards, E. Weimer, E. M. Scherer, N. Rouphael, S. Edupuganti, D. Weiskopf, L. V. Tse, Y. J. Hou, D. Margolis, A. Sette, M. H. Collins, J. Schmitz, R. S. Baric, A. M. de Silva, The receptor binding domain of the viral spike protein is an immunodominant and highly specific target of antibodies in SARS-CoV-2 patients. *Sci Immunol* **5**, (2020).

720 21. D. Esposito, J. Mehalko, M. Drew, K. Snead, V. Wall, T. Taylor, P. Frank, J. P. Denson,
721 M. Hong, G. Gulten, K. Sadtler, S. Messing, W. Gillette, Optimizing high-yield
722 production of SARS-CoV-2 soluble spike trimers for serology assays. *Protein Expr Purif*
723 **174**, 105686 (2020).
724 22. N. C. Dalvie, S. A. Rodriguez-Aponte, B. L. Hartwell, L. H. Tostanoski, A. M.
725 Biedermann, L. E. Crowell, K. Kaur, O. Kumru, L. Carter, J. Yu, A. Chang, K. McMahan,
726 T. Courant, C. Lebas, A. A. Lemnios, K. A. Rodrigues, M. Silva, R. S. Johnston, C. A.
727 Naranjo, M. K. Tracey, J. R. Brady, C. A. Whittaker, D. Yun, S. Kar, M. Porto, M. Lok,
728 H. Andersen, M. G. Lewis, K. R. Love, D. L. Camp, J. M. Silverman, H. Kleanthous, S.
729 B. Joshi, D. B. Volkin, P. M. Dubois, N. Collin, N. P. King, D. H. Barouch, D. J. Irvine, J.
730 C. Love, Engineered SARS-CoV-2 receptor binding domain improves immunogenicity in
731 mice and elicits protective immunity in hamsters. *bioRxiv*, (2021).
732 23. S. Yang, Y. Li, L. Dai, J. Wang, P. He, C. Li, X. Fang, C. Wang, X. Zhao, E. Huang, C.
733 Wu, Z. Zhong, F. Wang, X. Duan, S. Tian, L. Wu, Y. Liu, Y. Luo, Z. Chen, F. Li, J. Li,
734 X. Yu, H. Ren, L. Liu, S. Meng, J. Yan, Z. Hu, L. Gao, G. F. Gao, Safety and
735 immunogenicity of a recombinant tandem-repeat dimeric RBD-based protein subunit
736 vaccine (ZF2001) against COVID-19 in adults: two randomised, double-blind, placebo-
737 controlled, phase 1 and 2 trials. *Lancet Infect Dis*, (2021).
738 24. L. Dai, T. Zheng, K. Xu, Y. Han, L. Xu, E. Huang, Y. An, Y. Cheng, S. Li, M. Liu, M.
739 Yang, Y. Li, H. Cheng, Y. Yuan, W. Zhang, C. Ke, G. Wong, J. Qi, C. Qin, J. Yan, G. F.
740 Gao, A Universal Design of Betacoronavirus Vaccines against COVID-19, MERS, and
741 SARS. *Cell* **182**, 722-733.e711 (2020).

742 25. B. M. Hauser, M. Sangesland, E. C. Lam, J. Feldman, A. S. Yousif, T. M. Caradonna, A.
743 B. Balazs, D. Lingwood, A. G. Schmidt, Engineered receptor binding domain
744 immunogens elicit pan-coronavirus neutralizing antibodies. *bioRxiv*, (2020).
745 26. T. K. Tan, P. Rijal, R. Rahikainen, A. H. Keeble, L. Schimanski, S. Hussain, R. Harvey, J.
746 W. P. Hayes, J. C. Edwards, R. K. McLean, V. Martini, M. Pedrera, N. Thakur, C.
747 Conceicao, I. Dietrich, H. Shelton, A. Ludi, G. Wilsden, C. Browning, A. K. Zagrajek, D.
748 Bialy, S. Bhat, P. Stevenson-Leggett, P. Hollinghurst, M. Tully, K. Moffat, C. Chiu, R.
749 Waters, A. Gray, M. Azhar, V. Mioulet, J. Newman, A. S. Asfor, A. Burman, S. Crossley,
750 J. A. Hammond, E. Tchilian, B. Charleston, D. Bailey, T. J. Tuthill, S. P. Graham, H. M.
751 E. Duyvesteyn, T. Malinauskas, J. Huo, J. A. Tree, K. R. Buttigieg, R. J. Owens, M. W.
752 Carroll, R. S. Daniels, J. W. McCauley, D. I. Stuart, K. A. Huang, M. Howarth, A. R.
753 Townsend, A COVID-19 vaccine candidate using SpyCatcher multimerization of the
754 SARS-CoV-2 spike protein receptor-binding domain induces potent neutralising antibody
755 responses. *Nature communications* **12**, 542 (2021).
756 27. A. C. Walls, B. Fiala, A. Schäfer, S. Wrenn, M. N. Pham, M. Murphy, L. V. Tse, L.
757 Shehata, M. A. O'Connor, C. Chen, M. J. Navarro, M. C. Miranda, D. Pettie, R.
758 Ravichandran, J. C. Kraft, C. Ogohara, A. Palser, S. Chalk, E. C. Lee, K. Guerriero, E.
759 Kepl, C. M. Chow, C. Sydeman, E. A. Hodge, B. Brown, J. T. Fuller, K. H. Dinnon, 3rd,
760 L. E. Gralinski, S. R. Leist, K. L. Gully, T. B. Lewis, M. Guttman, H. Y. Chu, K. K. Lee,
761 D. H. Fuller, R. S. Baric, P. Kellam, L. Carter, M. Pepper, T. P. Sheahan, D. Veesler, N.
762 P. King, Elicitation of Potent Neutralizing Antibody Responses by Designed Protein
763 Nanoparticle Vaccines for SARS-CoV-2. *Cell* **183**, 1367-1382.e1317 (2020).

764 28. L. Yang, D. Tian, J.-b. Han, W. Fan, Y. Zhang, Y. Li, W. Sun, Y. Wei, X. Tian, D.-d. Yu,
765 X.-l. Feng, G. Cheng, Y.-t. Zheng, Y. Bi, W. Liu, A recombinant receptor-binding
766 domain in trimeric form generates completely protective immunity against SARS-CoV-2
767 infection in nonhuman primates. *bioRxiv*, 2021.2003.2030.437647 (2021).
768 29. L. He, X. Lin, Y. Wang, C. Abraham, C. Sou, T. Ngo, Y. Zhang, I. A. Wilson, J. Zhu,
769 Single-component, self-assembling, protein nanoparticles presenting the receptor binding
770 domain and stabilized spike as SARS-CoV-2 vaccine candidates. *Sci Adv* **7**, (2021).
771 30. S. G. Reed, M. Tomai, M. J. Gale, Jr., New horizons in adjuvants for vaccine
772 development. *Curr Opin Immunol* **65**, 97-101 (2020).
773 31. B. Pulendran, S. A. P, D. T. O'Hagan, Emerging concepts in the science of vaccine
774 adjuvants. *Nature reviews. Drug discovery*, 1-22 (2021).
775 32. D. T. O'Hagan, R. N. Lodaya, G. Lofano, The continued advance of vaccine adjuvants -
776 'we can work it out'. *Seminars in immunology* **50**, 101426 (2020).
777 33. H. Lal, A. L. Cunningham, O. Godeaux, R. Chlibek, J. Diez-Domingo, S. J. Hwang, M. J.
778 Levin, J. E. McElhaney, A. Poder, J. Puig-Barberà, T. Vesikari, D. Watanabe, L. Weckx,
779 T. Zahaf, T. C. Heineman, Efficacy of an adjuvanted herpes zoster subunit vaccine in
780 older adults. *The New England journal of medicine* **372**, 2087-2096 (2015).
781 34. A. L. Cunningham, H. Lal, M. Kovac, R. Chlibek, S. J. Hwang, J. Díez-Domingo, O.
782 Godeaux, M. J. Levin, J. E. McElhaney, J. Puig-Barberà, C. Vanden Abeele, T. Vesikari,
783 D. Watanabe, T. Zahaf, A. Ahonen, E. Athan, J. F. Barba-Gomez, L. Campora, F. de
784 Looze, H. J. Downey, W. Ghesquiere, I. Gorfinkel, T. Korhonen, E. Leung, S. A. McNeil,
785 L. Oostvogels, L. Rombo, J. Smetana, L. Weckx, W. Yeo, T. C. Heineman, Efficacy of

the Herpes Zoster Subunit Vaccine in Adults 70 Years of Age or Older. *The New England journal of medicine* **375**, 1019-1032 (2016).

35. S. R. Leist, K. H. Dinnon, 3rd, A. Schäfer, L. V. Tse, K. Okuda, Y. J. Hou, A. West, C. E. Edwards, W. Sanders, E. J. Fritch, K. L. Gully, T. Scobey, A. J. Brown, T. P. Sheahan, N. J. Moorman, R. C. Boucher, L. E. Gralinski, S. A. Montgomery, R. S. Baric, A Mouse-Adapted SARS-CoV-2 Induces Acute Lung Injury and Mortality in Standard Laboratory Mice. *Cell* **183**, 1070-1085.e1012 (2020).

36. K. Lederer, D. Castaño, D. Gómez Atria, T. H. Oguin, 3rd, S. Wang, T. B. Manzoni, H. Muramatsu, M. J. Hogan, F. Amanat, P. Cherubin, K. A. Lundgreen, Y. K. Tam, S. H. Y. Fan, L. C. Eisenlohr, I. Maillard, D. Weissman, P. Bates, F. Krammer, G. D. Sempowski, N. Pardi, M. Locci, SARS-CoV-2 mRNA Vaccines Foster Potent Antigen-Specific Germinal Center Responses Associated with Neutralizing Antibody Generation. *Immunity* **53**, 1281-1295.e1285 (2020).

37. J. G. Liang, D. Su, T. Z. Song, Y. Zeng, W. Huang, J. Wu, R. Xu, P. Luo, X. Yang, X. Zhang, S. Luo, Y. Liang, X. Li, J. Huang, Q. Wang, X. Huang, Q. Xu, M. Luo, A. Huang, D. Luo, C. Zhao, F. Yang, J. B. Han, Y. T. Zheng, P. Liang, S-Trimer, a COVID-19 subunit vaccine candidate, induces protective immunity in nonhuman primates. *Nature communications* **12**, 1346 (2021).

38. W. F. Garcia-Beltran, E. C. Lam, K. St Denis, A. D. Nitido, Z. H. Garcia, B. M. Hauser, J. Feldman, M. N. Pavlovic, D. J. Gregory, M. C. Poznansky, A. Sigal, A. G. Schmidt, A. J. Iafrate, V. Naranbhai, A. B. Balazs, Multiple SARS-CoV-2 variants escape neutralization by vaccine-induced humoral immunity. *Cell*, (2021).

39. A. Kuzmina, Y. Khalaila, O. Voloshin, A. Keren-Naus, L. Boehm-Cohen, Y. Raviv, Y. Shemer-Avni, E. Rosenberg, R. Taube, SARS-CoV-2 spike variants exhibit differential infectivity and neutralization resistance to convalescent or post-vaccination sera. *Cell host & microbe*, (2021).

40. X. Shen, H. Tang, R. Pajon, G. Smith, G. M. Glenn, W. Shi, B. Korber, D. C. Montefiori, Neutralization of SARS-CoV-2 Variants B.1.429 and B.1.351. *The New England journal of medicine*, (2021).

41. Z. Wang, F. Schmidt, Y. Weisblum, F. Muecksch, C. O. Barnes, S. Finkin, D. Schaefer-Babajew, M. Cipolla, C. Gaebler, J. A. Lieberman, T. Y. Oliveira, Z. Yang, M. E. Abernathy, K. E. Huey-Tubman, A. Hurley, M. Turroja, K. A. West, K. Gordon, K. G. Millard, V. Ramos, J. Da Silva, J. Xu, R. A. Colbert, R. Patel, J. Dizon, C. Unson-O'Brien, I. Shimeliovich, A. Gazumyan, M. Caskey, P. J. Bjorkman, R. Casellas, T. Hatziioannou, P. D. Bieniasz, M. C. Nussenzweig, mRNA vaccine-elicited antibodies to SARS-CoV-2 and circulating variants. *Nature* **592**, 616-622 (2021).

42. L. J. Abu-Raddad, H. Chemaitelly, A. A. Butt, Effectiveness of the BNT162b2 Covid-19 Vaccine against the B.1.1.7 and B.1.351 Variants. *The New England journal of medicine*, (2021).

43. A. Iwasaki, R. Medzhitov, Control of adaptive immunity by the innate immune system. *Nat Immunol* **16**, 343-353 (2015).

44. A. J. Pollard, E. M. Bijker, A guide to vaccinology: from basic principles to new developments. *Nature reviews. Immunology* **21**, 83-100 (2021).

45. S. M. Grant, M. Lou, L. Yao, R. N. Germain, A. J. Radtke, The lymph node at a glance - how spatial organization optimizes the immune response. *J Cell Sci* **133**, (2020).

831 46. S. E. Acton, C. Reis e Sousa, Dendritic cells in remodeling of lymph nodes during
832 immune responses. *Immunol Rev* **271**, 221-229 (2016).
833 47. E. J. Williamson, A. J. Walker, K. Bhaskaran, S. Bacon, C. Bates, C. E. Morton, H. J.
834 Curtis, A. Mehrkar, D. Evans, P. Inglesby, J. Cockburn, H. I. McDonald, B. MacKenna,
835 L. Tomlinson, I. J. Douglas, C. T. Rentsch, R. Mathur, A. Y. S. Wong, R. Grieve, D.
836 Harrison, H. Forbes, A. Schultze, R. Croker, J. Parry, F. Hester, S. Harper, R. Perera, S. J.
837 W. Evans, L. Smeeth, B. Goldacre, Factors associated with COVID-19-related death
838 using OpenSAFELY. *Nature* **584**, 430-436 (2020).
839 48. Centers for Disease Control and Prevention (CDC). COVID-19 Hospitalization and
840 Death by Age, Accessed Apr 3rd, 2021, 2021
841 49. P. J. Hotez, M. E. Bottazzi, Developing a low-cost and accessible COVID-19 vaccine for
842 global health. *PLoS Negl Trop Dis* **14**, e0008548 (2020).
843 50. K. McMahan, J. Yu, N. B. Mercado, C. Loos, L. H. Tostanoski, A. Chandrashekar, J. Liu,
844 L. Peter, C. Atyeo, A. Zhu, E. A. Bondzie, G. Dagotto, M. S. Gebre, C. Jacob-Dolan, Z.
845 Li, F. Nampanya, S. Patel, L. Pessaint, A. Van Ry, K. Blade, J. Yalley-Ogunro, M. Cabus,
846 R. Brown, A. Cook, E. Teow, H. Andersen, M. G. Lewis, D. A. Lauffenburger, G. Alter,
847 D. H. Barouch, Correlates of protection against SARS-CoV-2 in rhesus macaques.
848 *Nature*, (2020).
849 51. P. S. Arunachalam, A. C. Walls, N. Golden, C. Atyeo, S. Fischinger, C. Li, P. Aye, M. J.
850 Navarro, L. Lai, V. V. Edara, K. Röltgen, K. Rogers, L. Shirreff, D. E. Ferrell, S. Wrenn,
851 D. Pettie, J. C. Kraft, M. C. Miranda, E. Kepl, C. Sydeman, N. Brunette, M. Murphy, B.
852 Fiala, L. Carter, A. G. White, M. Trisal, C.-L. Hsieh, K. Russell-Lodrigue, C. Monjure, J.
853 Dufour, L. Doyle-Meyer, R. B. Bohm, N. J. Maness, C. Roy, J. A. Plante, K. S. Plante, A.

Zhu, M. J. Gorman, S. Shin, X. Shen, J. Fontenot, S. Gupta, D. T. O'Hagan, R. V. D. Most, R. Rappuoli, R. L. Coffman, D. Novack, J. S. McLellan, S. Subramaniam, D. Montefiori, S. D. Boyd, J. L. Flynn, G. Alter, F. Villinger, H. Kleanthous, J. Rappaport, M. Suthar, N. P. King, D. Veesler, B. Pulendran, Adjuvanting a subunit SARS-CoV-2 nanoparticle vaccine to induce protective immunity in non-human primates. *bioRxiv*, 2021.2002.2010.430696 (2021).

52. W. H. Chen, J. Wei, R. T. Kundu, R. Adhikari, Z. Liu, J. Lee, L. Versteeg, C. Poveda, B. Keegan, M. J. Villar, A. C. de Araujo Leao, J. A. Rivera, P. M. Gillespie, J. Pollet, U. Strych, B. Zhan, P. J. Hotez, M. E. Bottazzi, Genetic modification to design a stable yeast-expressed recombinant SARS-CoV-2 receptor binding domain as a COVID-19 vaccine candidate. *Biochim Biophys Acta Gen Subj* **1865**, 129893 (2021).

53. W. H. Chen, X. Tao, A. S. Agrawal, A. Algaissi, B. H. Peng, J. Pollet, U. Strych, M. E. Bottazzi, P. J. Hotez, S. Lustigman, L. Du, S. Jiang, C. K. Tseng, Yeast-expressed SARS-CoV recombinant receptor-binding domain (RBD219-N1) formulated with aluminum hydroxide induces protective immunity and reduces immune enhancement. *Vaccine* **38**, 7533-7541 (2020).

54. J. Pollet, W. H. Chen, L. Versteeg, B. Keegan, B. Zhan, J. Wei, Z. Liu, J. Lee, R. Kundu, R. Adhikari, C. Poveda, M. J. Villar, A. C. de Araujo Leao, J. Altieri Rivera, Z. Momin, P. M. Gillespie, J. T. Kimata, U. Strych, P. J. Hotez, M. E. Bottazzi, SARS□CoV-2 RBD219-N1C1: A yeast-expressed SARS-CoV-2 recombinant receptor-binding domain candidate vaccine stimulates virus neutralizing antibodies and T-cell immunity in mice. *Human vaccines & immunotherapeutics*, 1-11 (2021).

876 55. J. Paavonen, P. Naud, J. Salmerón, C. M. Wheeler, S. N. Chow, D. Apter, H. Kitchener,
877 X. Castellsague, J. C. Teixeira, S. R. Skinner, J. Hedrick, U. Jaisamrarn, G. Limson, S.
878 Garland, A. Szarewski, B. Romanowski, F. Y. Aoki, T. F. Schwarz, W. A. Poppe, F. X.
879 Bosch, D. Jenkins, K. Hardt, T. Zahaf, D. Descamps, F. Struyf, M. Lehtinen, G. Dubin,
880 Efficacy of human papillomavirus (HPV)-16/18 AS04-adjuvanted vaccine against
881 cervical infection and precancer caused by oncogenic HPV types (PATRICIA): final
882 analysis of a double-blind, randomised study in young women. *Lancet (London, England)*
883 **374**, 301-314 (2009).
884 56. J. D. Campbell, Development of the CpG Adjuvant 1018: A Case Study. *Methods in*
885 *molecular biology (Clifton, N.J.)* **1494**, 15-27 (2017).
886 57. C. L. Cooper, H. L. Davis, M. L. Morris, S. M. Efler, M. A. Adhami, A. M. Krieg, D. W.
887 Cameron, J. Heathcote, CPG 7909, an immunostimulatory TLR9 agonist
888 oligodeoxynucleotide, as adjuvant to Engerix-B HBV vaccine in healthy adults: a double-
889 blind phase I/II study. *J Clin Immunol* **24**, 693-701 (2004).
890 58. B. Maletto, A. Rópolo, V. Morón, M. C. Pistoresi-Palencia, CpG-DNA stimulates
891 cellular and humoral immunity and promotes Th1 differentiation in aged BALB/c mice.
892 *Journal of leukocyte biology* **72**, 447-454 (2002).
893 59. B. A. Maletto, A. S. Rópolo, M. V. Liscovsky, D. O. Alignani, M. Glocker, M. C.
894 Pistoresi-Palencia, CpG oligodeoxinucleotides functions as an effective adjuvant in aged
895 BALB/c mice. *Clinical immunology (Orlando, Fla.)* **117**, 251-261 (2005).
896 60. B. M. Manning, E. Y. Enioutina, D. M. Visic, A. D. Knudson, R. A. Daynes, CpG DNA
897 functions as an effective adjuvant for the induction of immune responses in aged mice.
898 *Exp Gerontol* **37**, 107-126 (2001).

899 61. F. Ming, J. Yang, P. Chu, M. Ma, J. Shi, H. Cai, C. Huang, H. Li, Z. Jiang, H. Wang, W.
900 Wang, S. Zhang, L. Zhang, Immunization of aged pigs with attenuated pseudorabies
901 virus vaccine combined with CpG oligodeoxynucleotide restores defective Th1 immune
902 responses. *PloS one* **8**, e65536 (2013).
903 62. W. Qin, J. Jiang, Q. Chen, N. Yang, Y. Wang, X. Wei, R. Ou, CpG ODN enhances
904 immunization effects of hepatitis B vaccine in aged mice. *Cell Mol Immunol* **1**, 148-152
905 (2004).
906 63. G. Sen, Q. Chen, C. M. Snapper, Immunization of aged mice with a pneumococcal
907 conjugate vaccine combined with an unmethylated CpG-containing oligodeoxynucleotide
908 restores defective immunoglobulin G antipolysaccharide responses and specific CD4+-T-
909 cell priming to young adult levels. *Infection and immunity* **74**, 2177-2186 (2006).
910 64. B. P. Sablan, D. J. Kim, N. G. Barzaga, W. C. Chow, M. Cho, S. H. Ahn, S. G. Hwang, J.
911 H. Lee, H. Namini, W. L. Heyward, Demonstration of safety and enhanced
912 seroprotection against hepatitis B with investigational HBsAg-1018 ISS vaccine
913 compared to a licensed hepatitis B vaccine. *Vaccine* **30**, 2689-2696 (2012).
914 65. J. M. Janssen, S. Jackson, W. L. Heyward, R. S. Janssen, Immunogenicity of an
915 investigational hepatitis B vaccine with a toll-like receptor 9 agonist adjuvant (HBsAg-
916 1018) compared with a licensed hepatitis B vaccine in subpopulations of healthy adults
917 18-70 years of age. *Vaccine* **33**, 3614-3618 (2015).
918 66. T. Y. Kuo, M. Y. Lin, R. L. Coffman, J. D. Campbell, P. Traquina, Y. J. Lin, L. T. Liu, J.
919 Cheng, Y. C. Wu, C. C. Wu, W. H. Tang, C. G. Huang, K. C. Tsao, C. Chen,
920 Development of CpG-adjuvanted stable prefusion SARS-CoV-2 spike antigen as a
921 subunit vaccine against COVID-19. *Sci Rep* **10**, 20085 (2020).

67. C.-E. Lien, Y.-J. Lin, C. Chen, W.-C. Lian, T.-Y. Kuo, J. D. Campbell, P. Traquina, M.-Y. Lin, L. T.-C. Liu, Y.-S. Chuang, H.-Y. Ko, C.-C. Liao, Y.-H. Chen, J.-T. Jan, C.-P. Sun, Y.-S. Lin, P.-Y. Wu, Y.-C. Wang, M.-H. Tao, Y.-L. Lin, CpG-adjuvanted stable prefusion SARS-CoV-2 spike protein protected hamsters from SARS-CoV-2 challenge. *bioRxiv*, 2021.2001.2007.425674 (2021).

68. N. Kayraklioglu, B. Horuluoglu, D. M. Klinman, CpG Oligonucleotides as Vaccine Adjuvants. *Methods in molecular biology (Clifton, N.J.)* **2197**, 51-85 (2021).

69. D. J. Dowling, S. D. van Haren, A. Scheid, I. Bergelson, D. Kim, C. J. Mancuso, W. Foppen, A. Ozonoff, L. Fresh, T. B. Theriot, A. A. Lackner, R. N. Fichorova, D. Smirnov, J. P. Vasilakos, J. M. Beaurline, M. A. Tomai, C. C. Midkiff, X. Alvarez, J. L. Blanchard, M. H. Gilbert, P. P. Aye, O. Levy, TLR7/8 adjuvant overcomes newborn hyporesponsiveness to pneumococcal conjugate vaccine at birth. *JCI insight* **2**, e91020 (2017).

70. C. Garrido, A. D. Curtis, M. Dennis, S. H. Pathak, H. Gao, D. Montefiori, M. Tomai, C. B. Fox, P. A. Kozlowski, T. Scobey, J. E. Munt, M. L. Mallroy, P. T. Saha, M. G. Hudgens, L. C. Lindesmith, R. S. Baric, O. M. Abiona, B. Graham, K. S. Corbett, D. Edwards, A. Carfi, G. Fouda, K. K. A. Van Rompay, K. De Paris, S. R. Permar, SARS-CoV-2 Vaccines Elicit Durable Immune Responses in Infant Rhesus Macaques. *bioRxiv*, 2021.2004.2005.438479 (2021).

71. K. Wu, A. Choi, M. Koch, S. Elbashir, L. Ma, D. Lee, A. Woods, C. Henry, C. Palandjian, A. Hill, J. Quinones, N. Nunna, S. O'Connell, A. B. McDermott, S. Falcone, E. Narayanan, T. Colpitts, H. Bennett, K. Corbett, R. Seder, B. S. Graham, G. B. Stewart-Jones, A. Carfi, D. K. Edwards, Variant SARS-CoV-2 mRNA vaccines confer broad

945 neutralization as primary or booster series in mice. *bioRxiv*, 2021.2004.2013.439482
946 (2021).
947 72. N. W. Baylor, W. Egan, P. Richman, Aluminum salts in vaccines--US perspective.
948 *Vaccine* **20 Suppl 3**, S18-23 (2002).
949 73. F. Borriello, C. Pietrasanta, J. C. Y. Lai, L. M. Walsh, P. Sharma, D. N. O'Driscoll, J.
950 Ramirez, S. Brightman, L. Pugni, F. Mosca, D. J. Burkhart, D. J. Dowling, O. Levy,
951 Identification and Characterization of Stimulator of Interferon Genes As a Robust
952 Adjuvant Target for Early Life Immunization. *Front Immunol* **8**, 1772 (2017).
953 74. C. W. Tan, W. N. Chia, X. Qin, P. Liu, M. I. Chen, C. Tiu, Z. Hu, V. C. Chen, B. E.
954 Young, W. R. Sia, Y. J. Tan, R. Foo, Y. Yi, D. C. Lye, D. E. Anderson, L. F. Wang, A
955 SARS-CoV-2 surrogate virus neutralization test based on antibody-mediated blockage of
956 ACE2-spike protein-protein interaction. *Nat Biotechnol* **38**, 1073-1078 (2020).
957 75. J. Yu, L. H. Tostanoski, L. Peter, N. B. Mercado, K. McMahan, S. H. Mahrokhian, J. P.
958 Nkolola, J. Liu, Z. Li, A. Chandrashekar, D. R. Martinez, C. Loos, C. Atyeo, S.
959 Fischinger, J. S. Burke, M. D. Slein, Y. Chen, A. Zuiani, F. J. N. Lelis, M. Travers, S.
960 Habibi, L. Pessaint, A. Van Ry, K. Blade, R. Brown, A. Cook, B. Finneyfrock, A.
961 Dodson, E. Teow, J. Velasco, R. Zahn, F. Wegmann, E. A. Bondzie, G. Dagotto, M. S.
962 Gebre, X. He, C. Jacob-Dolan, M. Kirilova, N. Kordana, Z. Lin, L. F. Maxfield, F.
963 Nampanya, R. Nityanandam, J. D. Ventura, H. Wan, Y. Cai, B. Chen, A. G. Schmidt, D.
964 R. Wesemann, R. S. Baric, G. Alter, H. Andersen, M. G. Lewis, D. H. Barouch, DNA
965 vaccine protection against SARS-CoV-2 in rhesus macaques. *Science* **369**, 806-811
966 (2020).

967 76. J. Yu, Z. Li, X. He, M. S. Gebre, E. A. Bondzie, H. Wan, C. Jacob-Dolan, D. R. Martinez,
968 J. P. Nkolola, R. S. Baric, D. H. Barouch, Deletion of the SARS-CoV-2 Spike
969 Cytoplasmic Tail Increases Infectivity in Pseudovirus Neutralization Assays. *Journal of*
970 *Virology*, JVI.00044-00021 (2021).
971 77. S. D. van Haren, D. J. Dowling, W. Foppen, D. Christensen, P. Andersen, S. G. Reed, R.
972 M. Hershberg, L. R. Baden, O. Levy, Age-Specific Adjuvant Synergy: Dual TLR7/8 and
973 Mincle Activation of Human Newborn Dendritic Cells Enables Th1 Polarization. *Journal*
974 *of immunology (Baltimore, Md. : 1950)* **197**, 4413-4424 (2016).
975 78. M. C. Berenbaum, Correlations between methods for measurement of synergy. *The*
976 *Journal of infectious diseases* **142**, 476-480 (1980).
977

ACKNOWLEDGEMENTS

We thank the members of the BCH *Precision Vaccine Program* for helpful discussions. We thank Drs. Kevin Churchwell, Gary Fleisher, David Williams, and Mr. August Cervini for their support of the *Precision Vaccines Program.* We thank Dr. Barney S. Graham (NIH Vaccine Research Center) for generously providing the plasmid for pre-fusion stabilized SARS-CoV-2 Spike trimer. We thank Dr. Ralph Baric for providing the SARS-CoV-2/MA10 virus. We thank the pharmacists of Boston Children's Hospital for their efforts to maximize the use of SARS-CoV-2 vaccines by saving leftover or overfill of otherwise to be discarded vaccine vials. D.J.D. would like to thank Ms. Siobhan McHugh, Ms. Geneva Boyer, Mrs. Lucy Conetta and the staff of Lucy's Daycare, the staff the YMCA of Greater Boston, Bridging Independent Living Together (BILT), Inc., and the Boston Public Schools for childcare and educational support during the COVID-19 pandemic.

FUNDING

The current study was supported in part by US National Institutes of Health (NIH)/National Institutes of Allergy and Infectious Diseases (NIAID) awards, including Adjuvant Discovery (HHSN272201400052C and 75N93019C00044) and Development (HHSN272201800047C) Program Contracts to O.L. D.J.D.'s laboratory is supported by NIH grant (1R21AI137932-01A1), Adjuvant Discovery Program contract (75N93019C00044). R.E.H. is supported by the U.S. Army's Long Term Health and Education Training Program and M.B.F. is partially supported by BARDA# ASPR-20-01495, DARPA# ASPR-20-01495, NIH R01 AI148166, and NIH HHSN272201400007C. A.G.S.'s laboratory is supported by NIH R01 AI146779 (A.G.S.), NIGMS T32 GM007753 (B.M.H. and T.M.C.), T32 AI007245 (J.F.), and a Massachusetts

1001 Consortium on Pathogenesis Readiness (MassCPR) grant to A.G.S. I.Z. is supported by NIH
1002 grants 1R01AI121066 and 1R01DK115217, and holds an Investigators in the Pathogenesis of
1003 Infectious Disease Award from the Burroughs Wellcome Fund. The *Precision Vaccines Program*
1004 is supported in part by the BCH Department of Pediatrics and the Chief Scientific Office. E.N. is
1005 supported by the Daiichi Sankyo Foundation of Life Science and Uehara Memorial Foundation
1006 and is a joint Society for Pediatric Research and Japanese Pediatric Society Scholar.
1007

1008 **AUTHOR CONTRIBUTIONS**

1009 EN and FB conceived, designed, performed, analyzed the experiments and wrote the paper; TRO,
1010 YS, BB, MDL, KC, MMe, SDG, and SVH performed *in vitro* and/or *in vivo* experiments and
1011 their analysis; JC and JD-A performed the analysis of the qPCR data; KS, AZX, HSS, SDP,
1012 TMC, JF, BMH, AGS expressed and purified SARS-CoV-2 RBD and Spike; MEM, REH, CD,
1013 SMW, RMJ, HLH, RM, AB and MBF performed and analyzed SARS-CoV-2 neutralization
1014 experiments and mouse challenge study; AC, JY and DHB performed and analyzed pseudovirus
1015 neutralization experiments; ACS and LRB contributed to the human elderly *in vitro* analysis;
1016 MEB, PJH, and US edited and critically reviewed the manuscript; RKE and IZ contributed to the
1017 design of experiments; AO provided design feedback and contributed to the statistical analysis;
1018 OL and DJD conceived the project, designed the experiments, supervised the study and wrote the
1019 paper.
1020

1021 **COMPETING INTERESTS STATEMENT**

1022 EN, FB, TRO, YS, SVH, OL, and DJD are named inventors on vaccine adjuvant patents
1023 assigned to Boston Children's Hospital. FB has signed consulting agreements with Merck

Sharp & Dohme Corp. (a subsidiary of Merck & Co., Inc.), Sana Biotechnology, Inc., and F. Hoffmann-La Roche Ltd. IZ reports compensation for consulting services with Implicit Biosciences. MF is on the advisory board of Aikido Pharma. The BCM authors declare they are developers of a recombinant RBD technology. Baylor College of Medicine recently licensed the technology to Biological E, an Indian manufacturer, for advancement and licensure. These commercial or financial relationships are unrelated to the current study.

DATA AND MATERIALS AVAILABILITY

All data are available in the main text or the supplementary materials

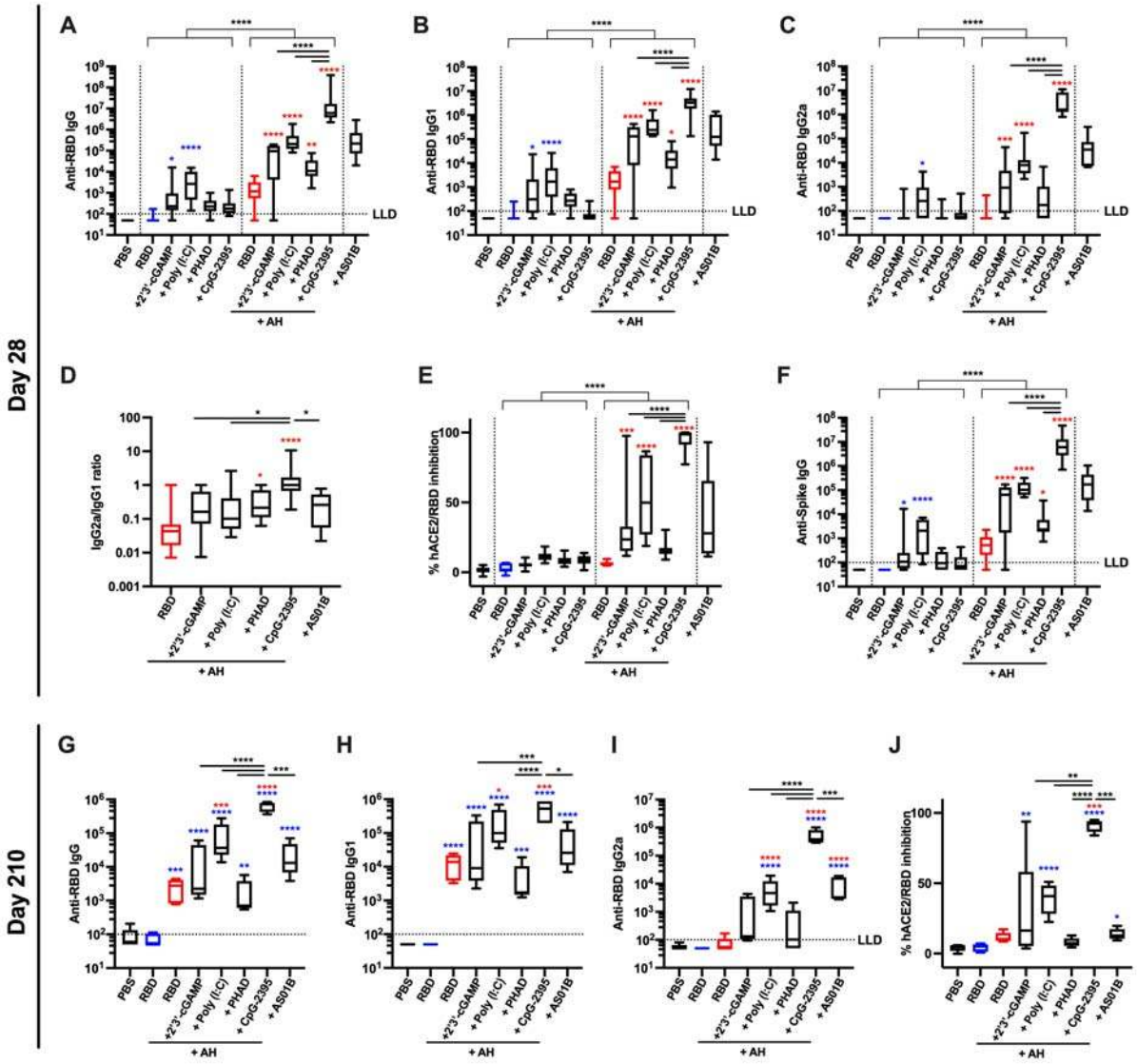

1034

1035 **Figure 1. RBD formulated with AH:CpG induces robust production of anti-RBD**

1036 **neutralizing antibodies in young adult mice**

1037 Young adult, 3-month-old BALB/c mice were immunized IM on Days 0 and 14 with 10 µg of

1038 monomeric SARS-CoV-2 RBD protein with indicated adjuvants. Each PRR agonist was

1039 administered alone or formulated with aluminum hydroxide (AH). (**A–F**) Serum samples were

1040 collected on Day 28, and (**A**) Anti-RBD IgG, (**B**) IgG1, (**C**) IgG2a, (**D**) IgG2a/IgG1 ratio, (**E**)

1041 hACE2/RBD inhibition rate, and (**F**) anti-Spike IgG were assessed. N=10 per group. Data were

combined from two individual experiments. (**G–J**) Serum samples were collected on Day 210, and (**G**) Anti-RBD IgG, (**H**) IgG1, (**I**) IgG2a and (**J**) hACE2/RBD inhibition rate were assessed. N=5 per group. Data were analyzed by two-way (**A–C, E–F**) (AH and PRR agonist) or one-way (**D, G–J**) ANOVAs followed by post-hoc Tukey's test for multiple comparisons. **P* <0.05, ***P* <0.01, ****P* <0.001, **** *P* <0.0001. Blue and red colored asterisks respectively indicate comparisons to RBD and AH adjuvanted RBD groups. Box-and-whisker plots represent the minimum, first quartile, median, third quartile, and maximum value. LLD, lower limit of detection.

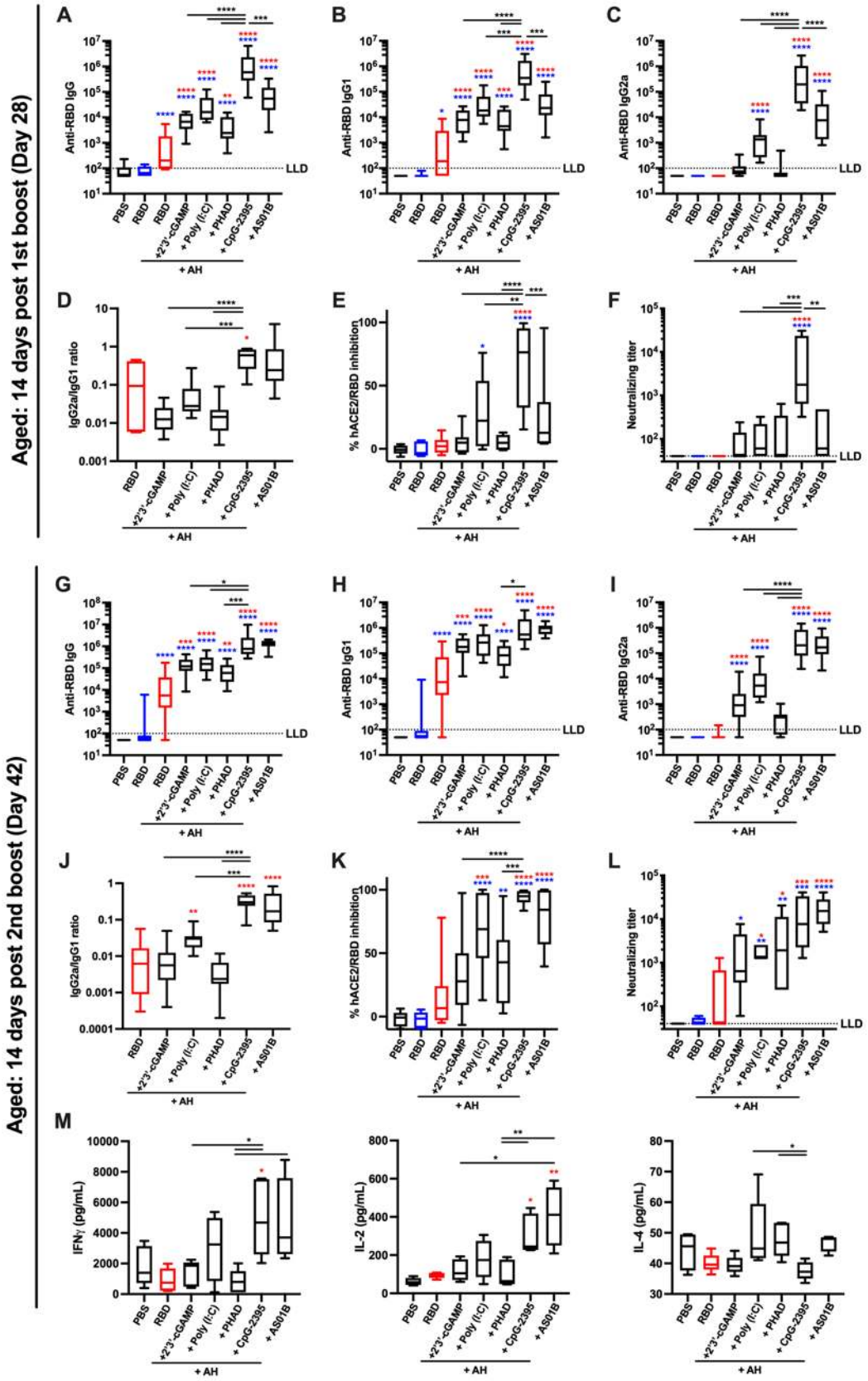

1050

Figure 2. AH:CpG adjuvant formulation elicits a robust anti-RBD response in aged mice

Aged, 14-month-old BALB/c mice were immunized IM on Days 0, 14, and 28 with 10 µg of monomeric SARS-CoV-2 RBD protein with indicated adjuvants. Each PRR agonist was formulated with aluminum hydroxide (AH). Serum samples were collected and analyzed on day 28 prior to the 2nd boost (**A–F**), and day 42 (**G–L**). (**A, G**) Anti-RBD IgG, (**B, H**) IgG1, (**C, I**) IgG2a, (**D, J**) IgG2a/IgG1 ratio, (**E, K**) hACE2/RBD inhibition rate, and (**F, L**) neutralizing titer were assessed. N=9–10 per group. Data were combined from two individual experiments and analyzed by one-way ANOVAs followed by post-hoc Tukey's test for multiple comparisons. (**M**) Splenocytes were collected 2 weeks after the final immunization and stimulated with a SARS-CoV 2 Spike peptide pool in the presence of anti-CD28 antibody (1 µg/mL). After 24 (for IL-2 and IL-4) and 96 (for IFNγ) hours, supernatants were harvested and cytokine levels were measured by ELISA. N=4-5 per group. Data were log-transformed and analyzed by one-way ANOVAs followed by post-hoc Tukey's test for multiple comparisons. **P* <0.05, ***P* <0.01, ****P* <0.001, **** *P* <0.0001. Blue and red colored asterisks respectively indicate comparisons to RBD and AH adjuvanted RBD groups. Box-and-whisker plots represent the minimum, first quartile, median, third quartile, and maximum value. LLD, lower limit of detection.

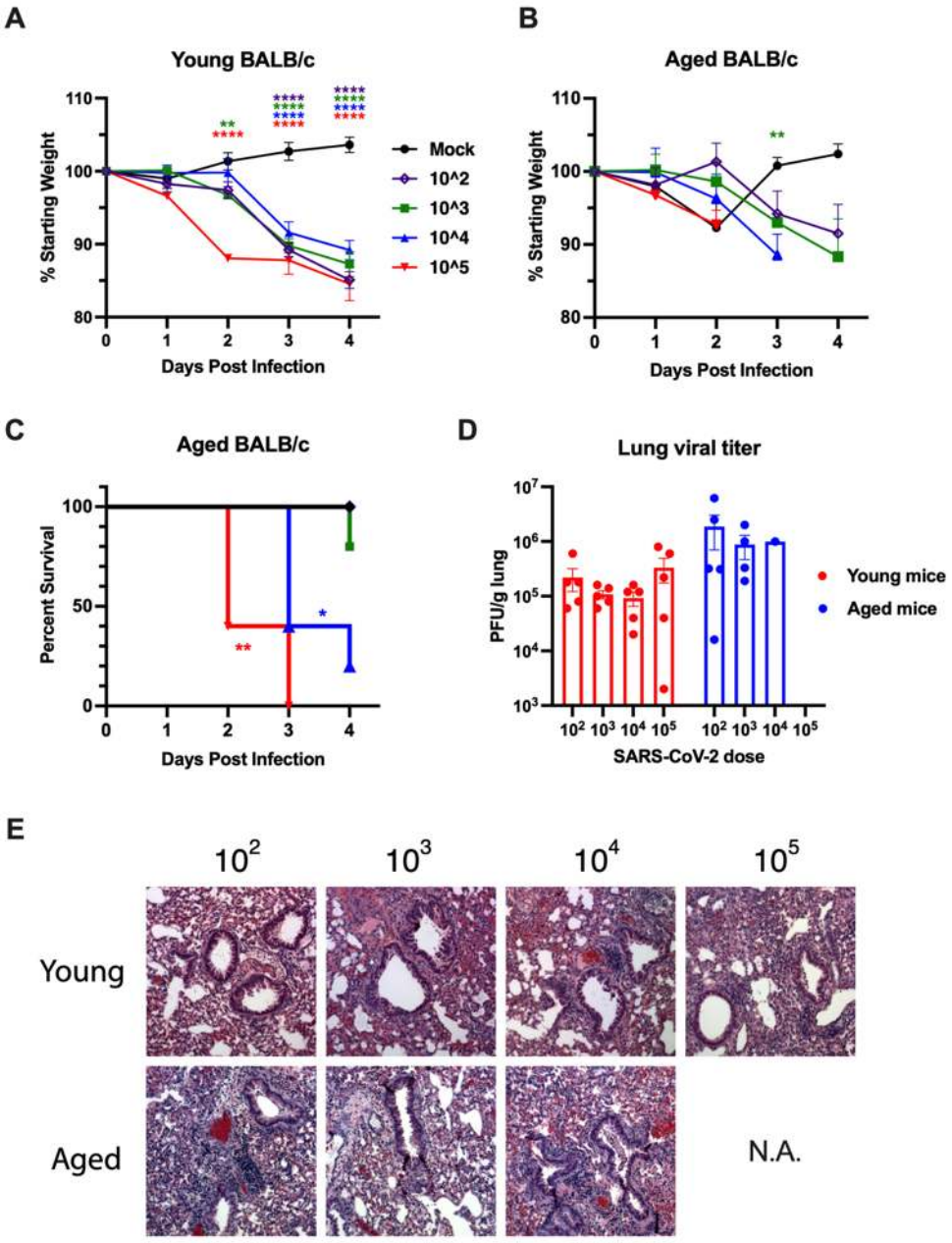

Figure 3. SARS-CoV-2 challenge model of young and aged mouse recapitulates human age-specific pathogenesis

Young (3-month-old) and aged (14-month-old) naïve BALB/c mice were challenged IN with mock (PBS), or 10^2, 10^3, 10^4, and 10^5 PFU of mouse-adapted SARS-CoV-2 (MA10). Bodyweight change of (**A**) young adult and (**B**) aged mice were assessed daily up to 4 days post infection. Data represent mean and SEM with body weights only shown for surviving mice at

each time-point. Data were analyzed by one-way ANOVA followed by Dunnett's test for comparisons against the PBS group. (**C**) Survival rate of aged mice. Data were analyzed by log-rank test in comparison to PBS group. (**D**) Viral titer in lung homogenates at 4-days post SARS-CoV-2 challenge (young: n=5 per group, aged: n=5 for 10^2; n=4 for 10^3; n=1 for 10^4; and n=0 for 10^5). Results represent mean ± SEM. (**E**) Representative lung histological images at 4-days post challenge. H&E is shown. **P* <0.05, ***P* <0.01, ****P* <0.001, **** *P* <0.0001.

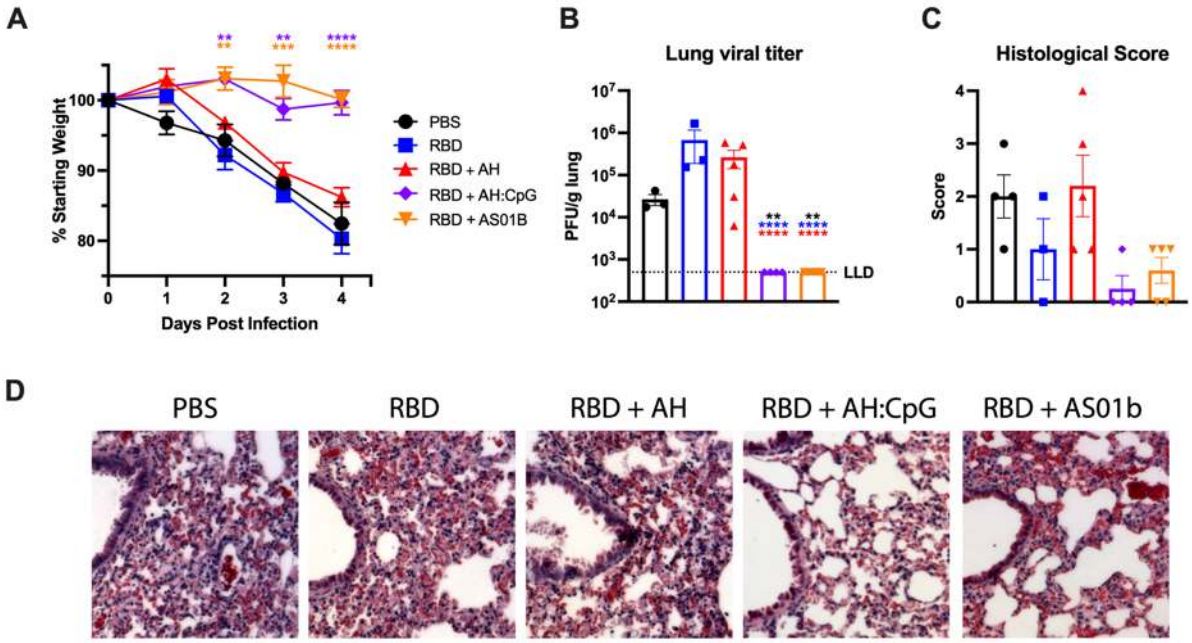

Figure 4. AH:CpG-adjuvanted vaccine protects aged mice from SARS-CoV-2 challenge

Aged, 14-month-old BALB/c mice were immunized as in **Figure 2**. On Day 70 (6 weeks post 2nd boost), mice were challenged IN with 10^3 PFU of mouse-adapted SARS-CoV-2 (MA10). (**A**) Bodyweight changes were assessed daily up to 4 days post infection. Data represent mean and SEM with body weights shown for surviving mice at each time-point (one mouse in RBD group died at 4 days post infection). Data were analyzed by one-way ANOVA followed by Dunnett's Test for comparisons between PBS group. (**B**) Viral titer in lung homogenates at 4-days post SARS-CoV-2 challenge. Results represent mean ± SEM. Data were analyzed by one-way ANOVA followed by post-hoc Tukey's test for multiple comparisons. $^{**}P < 0.01$, $^{****}P < 0.0001$. Black, blue and red colored asterisks respectively indicate comparisons to PBS, RBD, and RBD + aluminum hydroxide (AH) groups. LLD, lower limit of detection. (**C**) Lung interstitial inflammation was evaluated and converted to a score of 0-4 with 0 being no inflammation and 4 being most severe. (**D**) Representative lung histological images at 4-days post challenge. H&E is shown. N=4-5 animals per group.

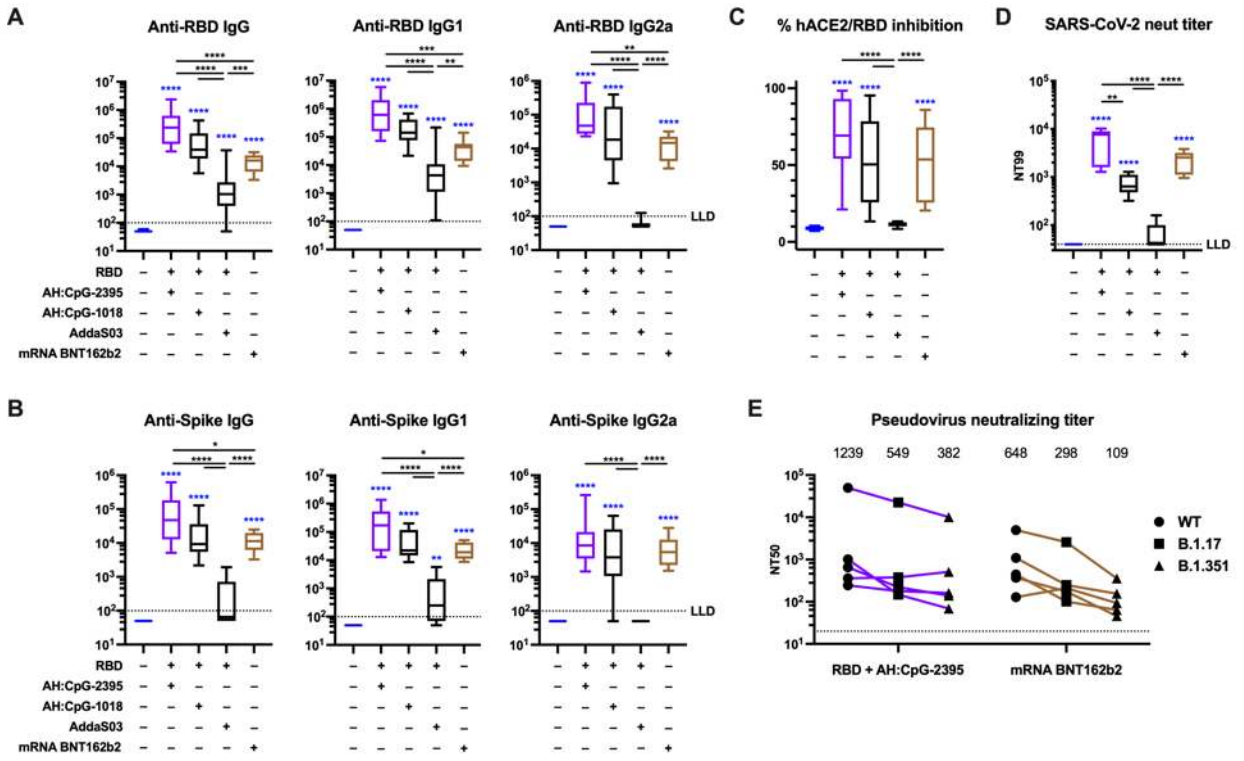

Figure 5. AH:CpG-adjuvanted RBD vaccines and an authorized spike mRNA vaccine elicit comparable levels of neutralizing antibodies in aged mice

Aged, 14-month-old BALB/c mice were immunized IM on Days 0 and 14 with monomeric SARS-CoV-2 RBD protein with indicated adjuvants, or BNT162b2 Spike mRNA vaccine as described in Methods. Serum samples were collected and analyzed on Day 28. (**A**) Anti-RBD binding ELISA, (**B**) anti-Spike binding ELISA, (**C**) hACE2/RBD inhibition rate, and (**D**) SARS-CoV-2 virus neutralizing titer were assessed. N=9–10 per group. Data were combined from two individual experiments and analyzed by one-way ANOVAs followed by post-hoc Tukey's test for multiple comparisons. (**E**) Pseudovirus neutralizing titers against wild-type or the B.1.17 or B.1.351 variants were assessed. N=5 per group. The numbers indicate GMT. Each symbol represents an animal. **P* <0.05, ***P* <0.01, ****P* <0.001, **** *P* <0.0001. Blue colored asterisks indicate comparisons to PBS group. Box-and-whisker plots represent the minimum, first quartile, median, third quartile, and maximum value. LLD, lower limit of detection.

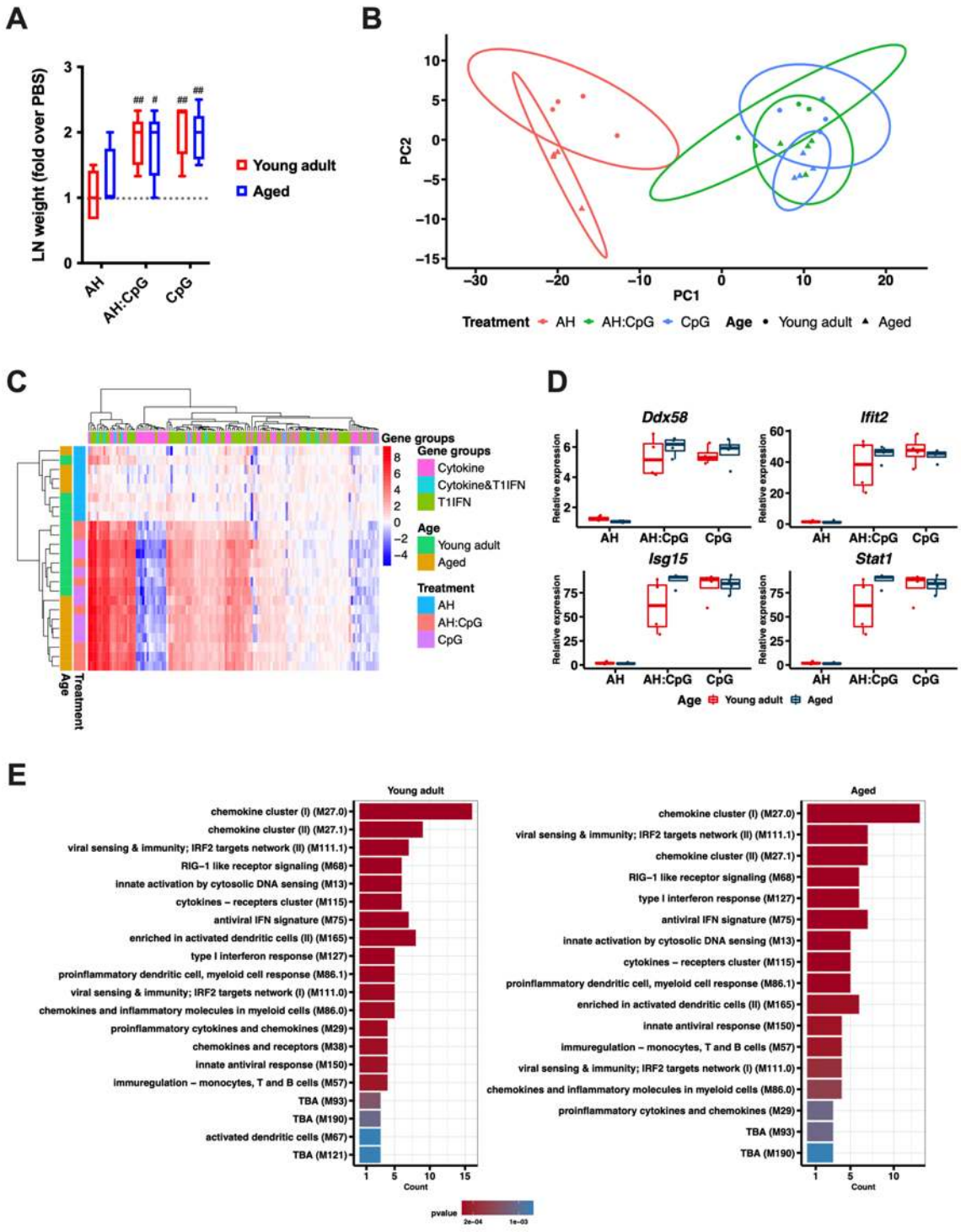

Figure 6. AH:CpG elicits comparable lymph node innate responses in young and aged mice

Young (3-month-old) and aged (14-month-old) mice were subcutaneously injected with aluminum hydroxide (AH), CpG, or AH:CpG. 24 hours later, draining lymph nodes (dLNs) were

collected and RNA was extracted. (**A**) Weights of dLNs were measured and expressed as fold over contralateral, PBS-injected LN. N=5 per group. # and ## respectively indicate P <0.05 and 0.01 when comparing each group against the value 1 (which represents the contralateral control sample expressed as fold). (**B–E**) RNA isolated from dLNs was subjected to a quantitative real-time PCR array comprised of 157 genes related to cytokines, chemokines, and type 1 IFN responses. N=4 animals per group. (**B**) Principal component analysis demonstrated a marked separation by treatment and age. (**C**) Unsupervised hierarchical clustering revealed major differences between treatments and highlighted the marked difference between AH and CpG-containing treatments. Each column represents gene categories and rows represent samples. (**D**) Generalized linear model comparing treatment and age with each gene was performed. The top 4 significant genes (*Ddx58*, *Ifit2*, *Isg15*, *Stat1*) were selected and plotted with their relative expression values by age and treatment. Statistical analysis of the plots employed the Kruskal-Wallis test to compare mean differences across groups and Wilcoxon test to compare between ages. (**E**) Enrichment analysis of differentially expressed genes using the blood transcriptional modules (Li et al., 2013- PMC: 24336226) was performed from the significant gene results after the generalized linear model by treatment. The top 20 modules are summarized per age.

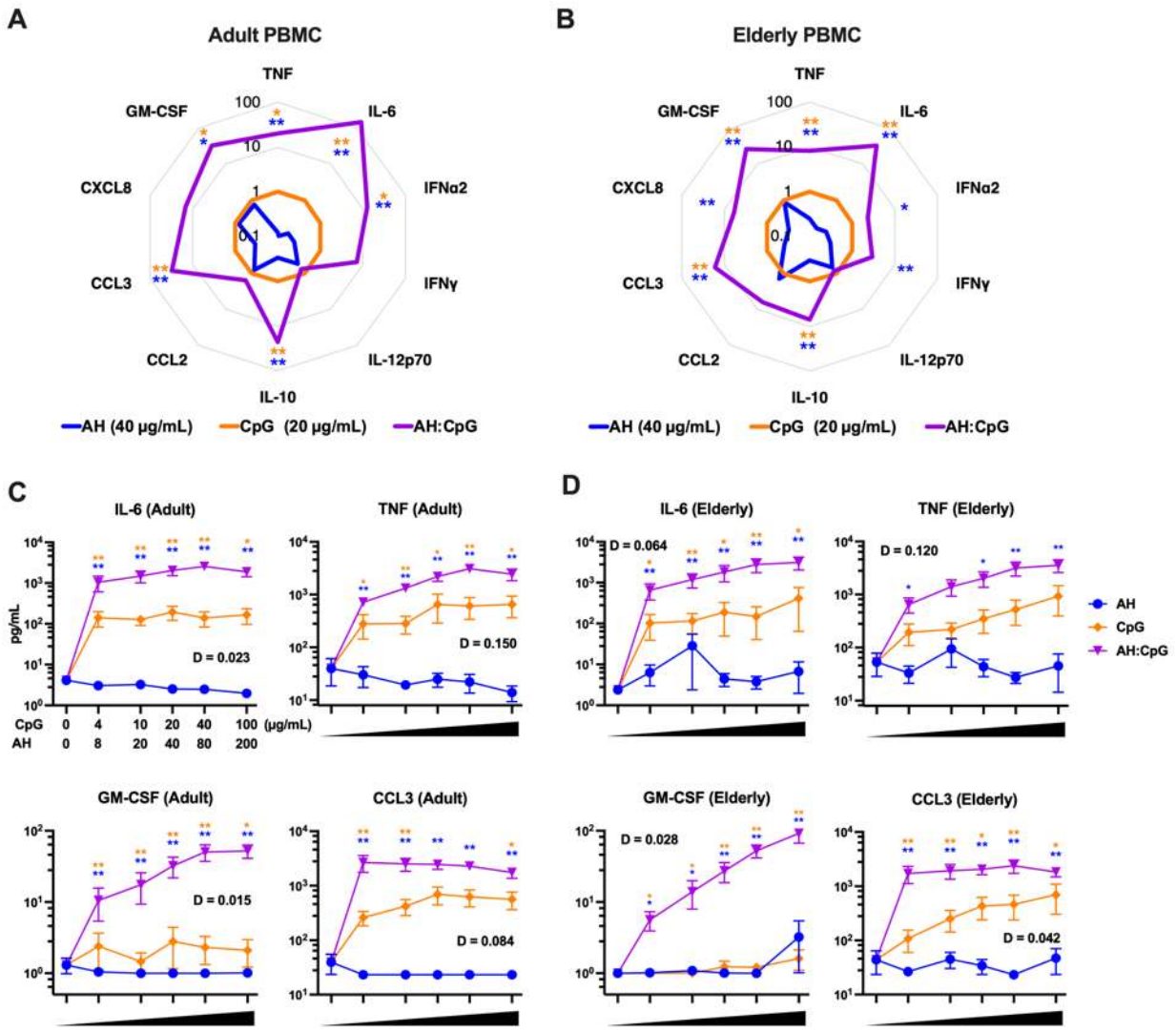

Figure 7. AH:CpG synergistically enhances proinflammatory cytokine production from human adult and elderly PBMCs

Human PBMCs collected from young adult (**A, C**) and elderly individuals (**B, D**) were cultured *in vitro* for 24 h with CpG alone (4, 10, 20, 40, and 100 µg/mL), aluminum hydroxide (AH) alone (8, 20, 40, 80, and 200 µg/mL), or a combination of both. Supernatants were collected for multiplexing bead array. N=6 per age group. (**A-B**) Radar plot analysis of cytokines and chemokines are presented as a fold-change over the CpG alone group for the 20 µg/mL CpG and 40 µg/mL AH conditions. (**C-D**) Results represent mean ± SEM. Unpaired Mann-Whitney tests were applied at each concentration. Blue and yellow colored asterisks indicate comparisons of

AH:CpG formulation to AH and CpG alone groups, respectively. *P <0.05, **P <0.01. Level of synergy was calculated using an adapted Loewe definition of additivity (D <1: synergy, D=1: additivity, D >1: antagonism).

1142 **SUPPLEMENTARY MATERIALS**

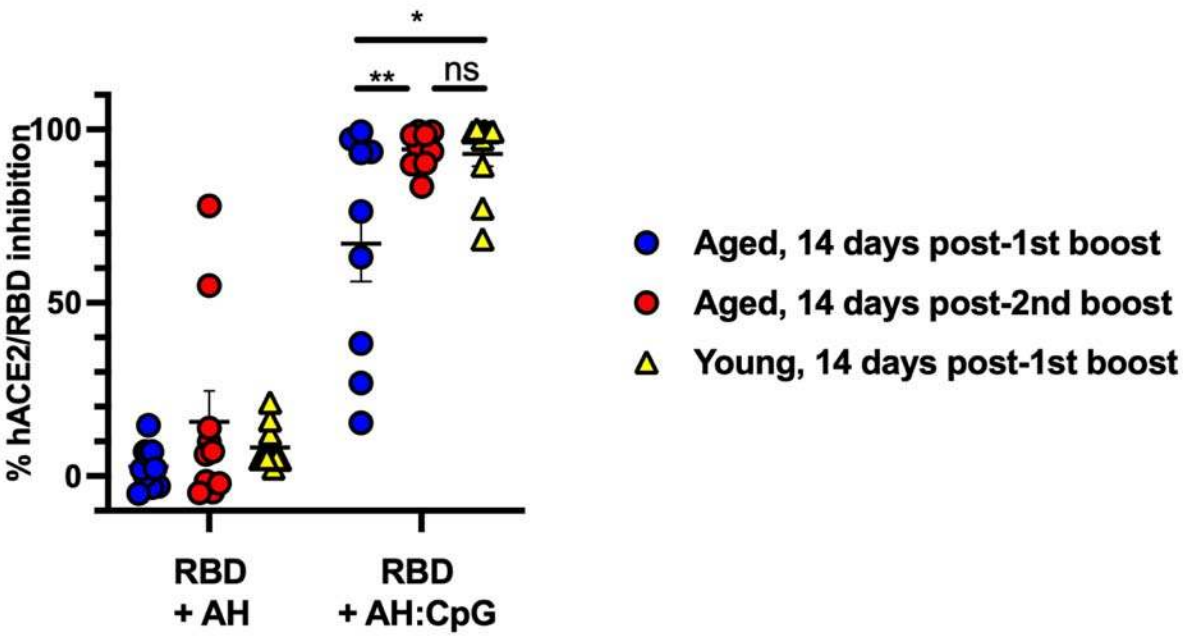

1143

1144 **Supplementary Figure 1. Booster dose of AH:CpG formulation enhances hACE2/RBD**

1145 **inhibition in aged mice**

1146 Young adult, 3-month-old BALB/c mice were immunized IM on Days 0 and 14, and aged, 14-

1147 month-old BALB/c mice were immunized IM on Days 0, 14, and 28 with 10 µg of monomeric

1148 SARS-CoV-2 RBD protein with the indicated adjuvants. Serum samples were collected and

1149 analyzed on Day 28 prior to the 2nd boost, and Day 42. hACE2/RBD inhibition rate was

1150 assessed. N = 9-10 animals per group. Data were combined from two individual experiments and

1151 analyzed by one-way ANOVA followed by post-hoc Tukey's test for multiple comparisons. Each

1152 dot represents individual results. Horizontal bars demonstrate mean plus SEM. ns: not significant,

1153 $*P$ <0.05, $**P$ <0.01. AH, aluminum hydroxide.

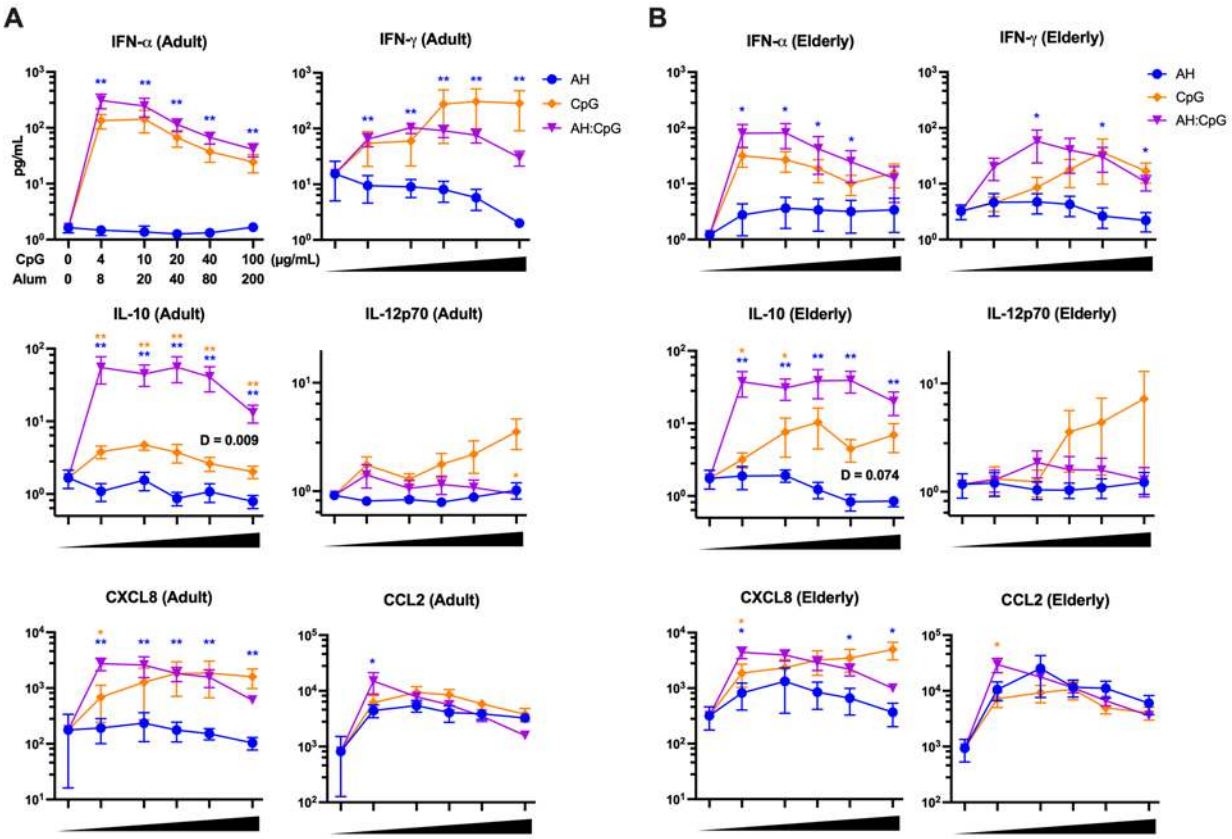

Supplementary Figure 2. AH and CpG synergistically induce cytokine and chemokine production by human young adult and elderly PBMCs

Human PBMCs collected from young adults (**A**) and elderly individuals (**B**) were cultured *in vitro* for 24 hrs with CpG alone (4, 10, 20, 40, and 100 μg/mL), aluminum hydroxide (AH) alone (8, 20, 40, 80, and 200 μg/mL), or combinations of each. Supernatants were collected for multiplexing bead array. N=6 per age group. Unpaired Mann-Whitney tests were applied at each concentration. Level of synergy was calculated using an adapted Loewe definition of additivity (D <1: synergy, D=1: additivity, D >1: antagonism). D value was not calculated if the concentration-dependent cytokine level did not fit a linear regression curve. Blue and yellow colored asterisks indicate comparisons of AH:CpG formulation to AH and CpG alone groups, respectively. Results represent mean ± SEM. **P* <0.05, ***P* <0.01.